

Kristoffer Vamråk Røed

Testing pressuremeter in sand

Master's thesis in Civil and Environmental Engineering

Supervisor: Ali Ghoreishian Amiri

June 2023

Kristoffer Vamråk Røed

Testing pressuremeter in sand

Master's thesis in Civil and Environmental Engineering
Supervisor: Ali Ghoreishian Amiri
June 2023

Norwegian University of Science and Technology
Faculty of Engineering
Department of Civil and Environmental Engineering



Preface

This is a master's thesis in geotechnics at NTNU, as a part of the MSc in Civil and Environmental Engineering was performed during the spring semester of 2023. This has been an interesting and challenging semester, with many practical hands-on tasks and exciting equipment. I have learned a lot about the difficulties of large-scale testing and the excitement when things finally work.

Trondheim, 11-06-2023

Kristoffer Vamråk Røed

Kristoffer Vamråk Røed

Acknowledgement

I would like to express my sincere gratitude to all those who have contributed to the completion of this master's thesis. Without their support, guidance, and assistance, this research would not have been possible.

First and foremost, I would like to thank my supervisor, Ali Ghoreishian Amiri, for his guidance and expertise throughout the entire research process. His feedback and dedication have been instrumental in shaping this thesis. I am truly grateful for his support.

I would also like to extend my appreciation to Espen Andersen Torsæter for his technical assistance and insights. His assistance during the data collection phase was invaluable.

Furthermore, I would like to thank my fellow classmates and friends for their support, stimulating discussions, and words of encouragement throughout this journey. Their friendship and camaraderie have been a source of inspiration and motivation.

Last but not least, I would like to express my heartfelt appreciation to my family and friends for their encouragement and belief in my abilities. Their constant support and understanding have been instrumental in my academic pursuits.

Summary

This study aimed to evaluate the quality of the pressuremeter system, and the accuracy of measurements obtained from pressuremeter testing. The pressuremeter is a valuable tool in geotechnical engineering for assessing soil properties. The rubber membrane of the pressuremeter demonstrated satisfactory behaviour, exhibiting elasticity, and returning to its original state after each test. However, issues were identified with the connections and tubes, resulting in small leaks that affected the system's ability to hold pressure. These leaks pose challenges for high-pressure or long-duration tests.

There were performed tests in sand with a relative density of 65% in a large chamber fulfilling the free field criterion. The pressuremeter was tested on medium-dense sand, performing Unloading-reloading loops, and interpreting the shear modulus of the sand. These results were compared to a Plaxis 2D simulation and Hardening soil parameters.

The accuracy of measurements obtained from the pressuremeter tests was influenced by various factors. The prototype pressuremeter used in this study measured the volume of water injected into the system, requiring assumptions about the radial strain and the expansion of the rubber membrane. Deviations from these assumptions introduced uncertainties and potential errors in the calculated soil parameters. Additionally, the presence of leaks and the viscoelastic properties of the rubber material impacted the pressure measurements. Discrepancies were observed between calculated shear moduli from hardening soil parameters previously calibrated for the tested soil, the shear modulus measured using the pressuremeter, and those interpreted from Plaxis2D simulation results. Further research and testing are necessary to establish correlations between measured and simulated shear moduli and to refine the interpretation of pressuremeter data.

Enhancing the quality of the pressuremeter system, particularly addressing the leaks in the connections and tubes, is crucial for improving its reliability. Improvements in accuracy can be achieved by refining assumptions and conducting additional tests at different depths. By addressing these aspects, the pressuremeter can become a more reliable tool for geotechnical design and analysis.

Sammendrag

Denne masteroppgaven hadde som mål å evaluere kvaliteten på et pressuremeter-systemet og nøyaktigheten av målinger oppnådd fra pressuremeter testingen. Et pressuremeter er et verdifullt verktøy innen geoteknisk design for vurdering av egenskapene til løsmassene. Gummimembranen til dette pressuremeteret viste tilfredsstillende oppførsel, med uniform og elastisk ekspansjon. Imidlertid ble det identifisert problemer med tilkoblingene og rørene, noe som førte til små lekkasjer som påvirket systemets evne til å holde trykket. Disse lekkasjene medfører utfordringer for tester med høyt trykk eller langvarige tester.

Det ble gjort tester i sand med en relativ tetthet på 65% i stort kammer som oppfylte kriteriet for testing uten påvirkning fra avgrensingen til kammeret. Det ble kjørt ekspansjon og kontraksjon av pressuremetert for så å tolke skjærmodulus fra disse resultatene. Deretter ble disse resultatene sammenliknet med resultater fra Plaxis 2D simulering og Hardening soil parametere.

Nøyaktigheten av målingene oppnådd fra testene ble påvirket av ulike faktorer. Prototypen som ble brukt studien, målte volumet av vann som ble injisert i systemet, og dette krever antagelser om radial deformasjon og ekspansjonen av gummimembranen. Avvik fra disse antagelsene medførte usikkerheter og mulige feil i beregnede jordparametere. I tillegg påvirket lekkasjene og de viskoelastiske egenskapene til gummimaterialet trykk-målingene.

Det ble observert avvik mellom beregnede skjærmoduler fra jordparametere i Hardening soil modellen, skjærmodulene tolket fra pressurmeter testene og de som ble tolket fra Plaxis2D-simuleringsresultater. Videre forskning og testing er nødvendig for å etablere korrelasjoner mellom målte og simulerte skjærmoduler og for å forbedre tolkningen av pressuremeter-data.

Forbedring av kvaliteten på pressuremeter-systemet, spesielt håndtering av lekkasjer i koblingene og rørene, er avgjørende for å forbedre dets pålitelighet. Forbedringer i nøyaktigheten kan oppnås ved å avgrense forutsetninger og utføre ytterligere tester på forskjellige dyp. Ved å adressere disse aspektene kan trykkmåleren bli et mer pålitelig verktøy for geoteknisk design og analyse.

Table of Contents

List of Figures	iv
List of Tables	vii
1 Introduction	1
1.1 Background	1
1.2 Objectives	2
1.3 Structure of the report	2
2 Theory	3
2.1 Testing chamber	3
2.1.1 Effect of the boundary conditions of the chamber on the pressuremeter tests	4
2.2 Properties of the sand	6
2.2.1 Grain size distribution	6
2.2.2 Grain density	6
2.2.3 Water content	7
2.2.4 Porosity limits and density	7
2.2.5 Triaxial tests	7
2.2.6 Summary of soil properties	10
2.3 Interpreting shear modulus G	11
3 Testing procedure	13
3.1 Initial testing of the equipment	13
3.1.1 Materials, equipment, and test setup	13

3.1.2	Initial measurement before testing	14
3.1.3	Removing the air and checking for leaks	14
3.1.4	Expansion test in the air; Stress-controlled	15
3.1.5	Expansion test in the air; Strain-controlled	15
3.1.6	Expansion test in the air; Strain-controlled with unload-reload loops	16
3.1.7	Expansion test in soil; Stress-controlled	17
3.1.8	Expansion test in the soil; Strain-controlled	18
3.2	Pressuremeter test in sand in large chamber	18
3.2.1	Materials, equipment, and test setup	18
3.2.2	Procedure	19
3.3	Pressuremeter test in air with Unloading-reloading loops	21
3.4	Simulating the pressuremeter test in Plaxis 2D	21
4	Results	24
4.1	Results from initial tests	24
4.1.1	Expansion test in the air; Stress-controlled	24
4.1.2	Expansion test in the air; Strain-controlled	26
4.1.3	Expansion test in the air; Strain-controlled with unload-reload loops	27
4.1.4	Expansion test in soil; Stress-controlled	29
4.1.5	Expansion test in the soil; Strain-controlled	31
4.2	Pressuremeter test in large chamber	33
4.2.1	Unloading-Reloading stiffness	34
4.2.2	Correction factor from tests in air	36
4.2.3	Corrected measurements of shear modulus	37
4.3	Plaxis 2D simulation of pressuremeter	40
4.3.1	Comparison between measured values and Plaxis 2D	40
5	Discussion	42
5.1	Quality of the pressuremeter	42

5.2 Accuracy of measurements	44
6 Conclusion	46
7 Recommendation for further work	48
7.1 Leakage	48
7.2 Rate of volumetric change	48
7.3 Correlation factor	48
Bibliography	49

List of Figures

2.1	Testing chamber cross section (Søvik 2017)	4
2.2	Schematic of boundary conditions (Mehdi-Ahmadi and Karambakhsh 2009)	5
2.3	Definition of loose, medium dense and dense sand (Mehdi-Ahmadi and Karambakhsh 2009)	5
2.4	Grain size distribution	6
2.5	Triaxial test with a confining pressure of 20 kPa and relative density of 66.7% (Søvik 2017)	8
2.6	Triaxial test with a confining pressure of 30 kPa and relative density of 59.1% (Søvik 2017)	9
2.7	Triaxial- and Soil test with a relative density of 67% and confining pressure 20 kPa (Søvik 2017)	10
2.8	Triaxial- and Soil test with a relative density of 59% and confining pressure 30 kPa (Søvik 2017)	10
2.9	The selection of shear moduli from an unload-reload cycle showing (a) the unload and reload secant moduli and (b) the nonlinear profile. G_{ur} = secant modulus from whole cycle; G_u = secant unload modulus measured from maximum cavity strain; G_r , = secant reload modulus measured from minimum cavity strain. (Clarke 1997)	12
3.1	Setup schematic	14
3.2	Measure points along the test tool	14
3.3	Example of applied pressure vs radial strain in a pressuremeter test	17
3.4	Screenshot of the program used to control the pump and log the results of the pressuremeter test	19
3.5	Model of how the axisymmetric model works in Plaxis2D (<i>Plaxis 2D</i> 2023)	22
3.6	Model of pressuremeter in Plaxis2D	23

4.1	Change in the diameter of the rubber bellow, Shore 50, during test 7.2	24
4.2	Change in pressure inside the rubber bellow, Shore 50, during test 7.2	25
4.3	Change in the diameter of the rubber bellow, Shore 70, during test 7.2	25
4.4	Change in pressure inside the rubber bellow, Shore 70, during test 7.2	25
4.5	Change in the diameter of the rubber bellow, Shore 50, during test 7.3	26
4.6	Change in pressure inside the rubber bellow, Shore 50, during test 7.3	26
4.7	Change in the diameter of the rubber bellow, Shore 70, during test 7.3	27
4.8	Change in pressure inside the rubber bellow, Shore 70, during test 7.3	27
4.9	Change in the diameter of the rubber bellow, Shore 50, during test 7.4	28
4.10	Change in pressure inside the rubber bellow, Shore 50, during test 7.4	28
4.11	Change in the diameter of the rubber bellow, Shore 70, during test 7.4	29
4.12	Change in pressure inside the rubber bellow, Shore 70, during test 7.4	29
4.13	Change in the diameter of the rubber bellow, Shore 50, during test 7.5	30
4.14	Change in pressure inside the rubber bellow, Shore 50, during test 7.5	30
4.15	Change in the diameter of the rubber bellow, Shore 70, during test 7.5	31
4.16	Change in pressure inside the rubber bellow, Shore 70, during test 7.5	31
4.17	Change in the diameter of the rubber bellow, Shore 50, during test 7.6	32
4.18	Change in pressure inside the rubber bellow, Shore 50, during test 7.6	32
4.19	Change in the diameter of the rubber bellow, Shore 70, during test 7.6	33
4.20	Change in pressure inside the rubber bellow, Shore 70, during test 7.6	33
4.21	Plot of unloading reloading loops test 1, on the y-axis the pressure P[kPa] inside the pressuremeter and on the x-axis $\epsilon_\theta = \frac{\Delta R}{R_0}$	34
4.22	Plot of unloading reloading loops test 2, on the y-axis the pressure P[kPa] inside the pressuremeter and on the x-axis $\epsilon_\theta = \frac{\Delta R}{R_0}$	35
4.23	Plot of unloading reloading loops test 3, on the y-axis the pressure P[kPa] inside the pressuremeter and on the x-axis $\epsilon_\theta = \frac{\Delta R}{R_0}$	35
4.24	Plot of unloading reloading loops test 4, on the y-axis the pressure P[kPa] inside the pressuremeter and on the x-axis $\epsilon_\theta = \frac{\Delta R}{R_0}$	36
4.25	Plot of unloading reloading loops, on the y-axis the pressure P[kPa] inside the pressuremeter and on the x-axis $\epsilon_\theta = \frac{\Delta R}{R_0}$	37
4.26	Plot of corrected unloading reloading loops, on the y-axis the pressure P[kPa] inside the pressuremeter and on the x-axis $\epsilon_\theta = \frac{\Delta R}{R_0}$	38

4.27	Plot of corrected unloading reloading loops, on the y-axis the pressure P[kPa] inside the pressuremeter and on the x-axis $\epsilon_\theta = \frac{\Delta R}{R_0}$	38
4.28	Plot of corrected unloading reloading loops, on the y-axis the pressure P[kPa] inside the pressuremeter and on the x-axis $\epsilon_\theta = \frac{\Delta R}{R_0}$	39
4.29	Plot of corrected unloading reloading loops, on the y-axis the pressure P[kPa] inside the pressuremeter and on the x-axis $\epsilon_\theta = \frac{\Delta R}{R_0}$	39
4.30	Plot of unloading reloading loops, on the y-axis the pressure P[kPa] inside the pressuremeter and on the x-axis $\epsilon_\theta = \frac{\Delta R}{R_0}$	40
4.31	Plot of unloading reloading loops, on the y-axis the pressure P[kPa] inside the pressuremeter and on the x-axis $\epsilon_\theta = \frac{\Delta R}{R_0}$	41
5.1	Measurement of pressure over time inside the pressuremeter while the chamber was being filled with sand	43
5.2	Measurement of pressure over time inside the pressuremeter	43
5.3	Plot of unloading-reloading loops in air, on the y-axis the pressure P[kPa] inside the pressuremeter and on the x-axis $\epsilon_\theta = \frac{\Delta R}{R_0}$	44

List of Tables

2.1	Index test summary. (Søvik 2017)	10
2.2	Hardening Soil parameters summary. (Søvik 2017)	11
3.1	Volumes changes calculated from diameter measurements of unloading reloading loops in the initial tests	20
3.2	Measurements of the diameter [mm] at different strain levels during the initial tests	20
4.1	Shear modulus G_{Uncorr} calculated from uncorrected unloading-reloading loops from pressuremeter test in soil	36
4.2	Shear modulus G_{ur} and G_u calculated from corrected unloading-reloading loops from pressuremeter test in soil	40
4.3	Comparison of shear modulus G_u from all tests	41

Symbols

OCR - Over consolidation ratio

E_{50}^{ref} - The reference secant modulus at 50% deviatoric stress in drained triaxial test.

E_{OED}^{ref} - Reference modulus for primary compression in oedometer conditions.

E_{ur}^{ref} - Reference modulus for unloading/reloading in drained triaxial test

K_0^{NC} - Earth pressure coefficient for normally consolidated material

K_0 - Earth pressure coefficient for over consolidated material

ϕ, ψ, c - Friction angle, dilatancy angle and cohesion at failure

ν_{ur} - Poisson' ratio for unloading/reloading

$e_{init}, e_{min}, e_{maz}$ - Void ratio input for dilatancy cut-off

m - Modulus exponent

p_{ref} - 100kPa

E_M - the Menard modulus calculated from the pressuremeter results using a $\nu = 0.33$

E - Young's modulus

$\alpha - \frac{E_M}{E}$

$\epsilon_\theta - \frac{\Delta R}{R_0}$

G_{Uncorr} - half the inclination of the unloading-reloading loop performed by the pressuremeter without correction for the stiffness of the pressuremeter

G_{ur} - half the inclination of the unloading-reloading loop performed by the pressuremeter with correction for the stiffness of the pressuremeter

G_u - half the inclination of the unloading section performed by the pressuremeter with correction for the stiffness of the pressuremeter

γ - density of the soil

σ'_3 - effective horizontal stress

Chapter 1

Introduction

In this thesis, the performance and quality of a new pressuremeter will be evaluated through tests in sand in a large chamber. The focus of the thesis is on the accuracy and usability of this new pressuremeter as an instrument in geotechnical engineering. In this context, the preparation of the soil sample in the chamber and the quality of the measurements will be examined thoroughly.

1.1 Background

The modern use of the pressuremeter test can be credited to the work of Louis Menard, a French engineer who refined the original concept developed by Kogler in the late 1950s, making it a practical testing instrument. (Winter 1987) Menard recognized the need for empirical methods to analyze foundation performance using the pressuremeter and conducted extensive full-scale measurements to establish empirical correlations. (Winter 1987)

The pressuremeter test involves the expansion of a membrane in a predrilled borehole, with a push-in pressuremeter or a selfboring pressuremeter, with measurements taken of volume change and pressure. (Winter 1987) Pressure is applied in predetermined steps, and a modulus is calculated to characterize the relationship between volume change and pressure. (Winter 1987) The pressure at which soil failure occurs, known as the limit pressure, is also evaluated. (Winter 1987) These two parameters, the pressuremeter modulus and limit pressure, along with the pressure-volume curve, are used for evaluations in geotechnical engineering design. (Winter 1987)

A company called Exceed Engineering has developed a new pressuremeter. It consists of a vulcanized rubber sleeve available in two different stiffnesses, shore 50 and shore 70. It is deformed using pressurized water. The pressure in the system and water pumped in and out are continuously measured. This pressuremeter was designed to be fitted to the back of a CPTU unit and used in offshore field testing. The purpose of the pressuremeter was to have a field testing device capable of finding the stiffness of the soil and the in situ stress condition. The most common way of finding the stiffness is to take out soil samples and test them in a Triax and Oedo-

meter machine, but this is both difficult and expensive. The finished version of the pressuremeter will have devices capable of measuring the displacement of the rubber sleeve and the pressure in the system. The pressuremeter tested in this thesis did not have any such devices and consisted solely of the metal frame and the rubber sleeve. All the results were recorded using a pump system measuring the pressure and the injected volume of water. The increase in radius was approximated based on the injected volume of water and the assumption that the pressuremeter expanded and contracted as a cylinder with a constant height and a uniform change in radius.

1.2 Objectives

The new device was tested in two different ways, initially, the rubber membrane was tested to verify that it doesn't deform plastically or deform unevenly during any type of soil investigation. In the main test, the pressuremeter was used to figure out the shear modulus of the soil by performing unloading and reloading loops. The purpose of these tests was to figure out:

1. If the quality of the materials used in the pressuremeter was good enough to be used in geotechnical design.
2. If the system connecting the pressuremeter to the surface works well enough or if it should be upgraded or changed in any way for future tests.
3. If the pressuremeter, in the state it is, could be used to collect data that could be used in geotechnical design.

1.3 Structure of the report

The thesis is structured as follows:

Chapter 2- Theories and information gathered from other studies relevant to this thesis

Chapter 3- The procedures of all the tests performed in the data-gathering stage of this thesis

Chapter 4- Results from the procedures described in Chapter 3 and interpretations of these

Chapter 5 Discussion on the results and comments in regard to the objectives of the thesis

Chapter 2

Theory

In this thesis, the soil sample refers to the soil surrounding the pressuremeter and consists of sand, which characteristics will be further discussed. The effects of testing in a chamber compared to testing in the field will be discussed, along with how the shear modulus of the sand was interpreted.

2.1 Testing chamber

The chamber used during the tests was previously used to test piles and was made to be emptied and filled automatically. It was filled using a large container moving back and forth, at a given speed, over the chamber, called a raining system. The amount of sand filled into the chamber each pass-over was controlled by the size of the holes underneath this container, which size could be changed, and by the speed it moved. That way it was also possible to control the density of the sand to some degree. The cross-section of this chamber is shown in Figure 2.1 as well as how the filling and emptying of the tank happened. The chamber was 4 meters wide in both directions and 3 meters deep.

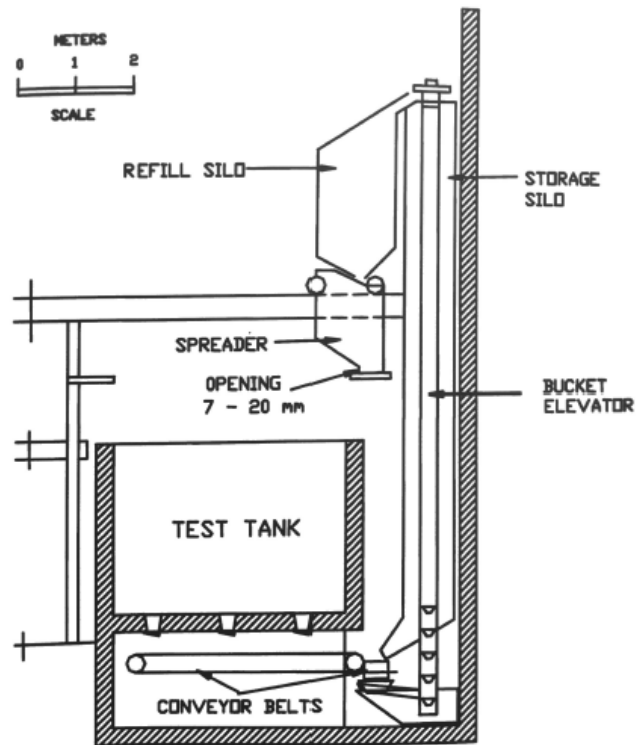


Figure 2.1: Testing chamber cross section (Søvik 2017)

2.1.1 Effect of the boundary conditions of the chamber on the pressuremeter tests

The pressuremeter tests were performed in a square chamber with a length of 400cm. While the maximum radius of the pressuremeter was 3.1cm, shown as r_c in Figure 2.2. One of the issues when performing tests in a confined chamber compared to performing them out in the field is how the boundary of the chamber interferes with the results. This raised the question, at what ratio R_d between R_c and r_c would the boundary of the chamber no longer interfere with the pressuremeter tests?

Mehdi-Ahmadi and Karambakhsh 2009 used a numerical model to calculate at what radius the chamber no longer interfered with the limit pressure calculated from the pressuremeter test. The article modeled the pressuremeter test as a typical axisymmetric cavity expansion problem with boundary conditions defined as shown in Figure 2.2. The Mohr-Coulomb model was used to define the soil in the problem. An initial vertical stress of 100 kPa and an initial horizontal stress of 50 kPa were used, and a coefficient of earth pressure at rest was equal to 0.5. This model was compared to experimental data from another study and concluded that the model agrees well with the experimental data.

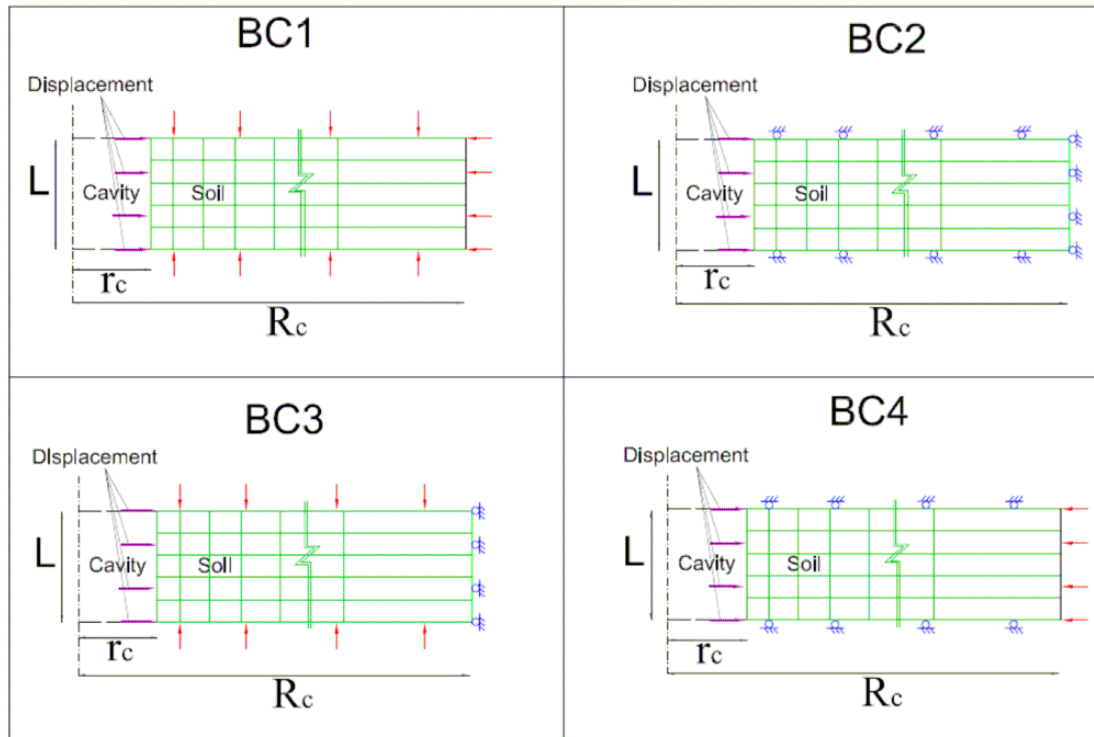


Figure 2.2: Schematic of boundary conditions (Mehdi-Ahmadi and Karambakhsh 2009)

The results of the model stated that loose, medium dense, and dense sand, which is defined in Figure 2.3, had different ratios at which the boundary no longer interfered with the limit pressure.

Sand state	D_r	K_G	K_B
Loose	45 %	195	325
Medium dense	65 %	230	385
Dense	85 %	290	480

Figure 2.3: Definition of loose, medium dense and dense sand (Mehdi-Ahmadi and Karambakhsh 2009)

The model was run using a R_d , defined in Equation 2.1, of between 10 and 500. The paper concluded that for loose sand the R_d needed to fulfill the free field criterion was 40. The free field criterion was the value R_d at which the boundary of the testing chamber no longer interfered with the pressuremeter tests. For medium-dense sand, R_d was 60, and for dense sand, it was 80.

$$R_d = \frac{R_c}{r_c} \quad (2.1)$$

This meant that the pressuremeter tested in this paper using medium-dense sand, with a radius r_c equal to 31mm at maximum inflation, needed a chamber with a radius of at least 1860 mm. In the square chamber, the minimum distance from the wall to the pressuremeter was 2000 mm, which means the free field criterion was fulfilled for both loose and medium-dense sand.

2.2 Properties of the sand

The sand used in this paper has previously been used in different masters and Ph.D. theses. The most recent was (Søvik 2017), in which different tests were performed to determine the characteristics of the sand. The same speed and hole size in the rainer system was used during this thesis, so the properties were expected to be almost identical. The results from (Søvik 2017) will be presented below.

2.2.1 Grain size distribution

The grain size distribution was found according to procedures described in ISO 17892-4:2016, and the result is shown in Figure 2.4. (Søvik 2017)

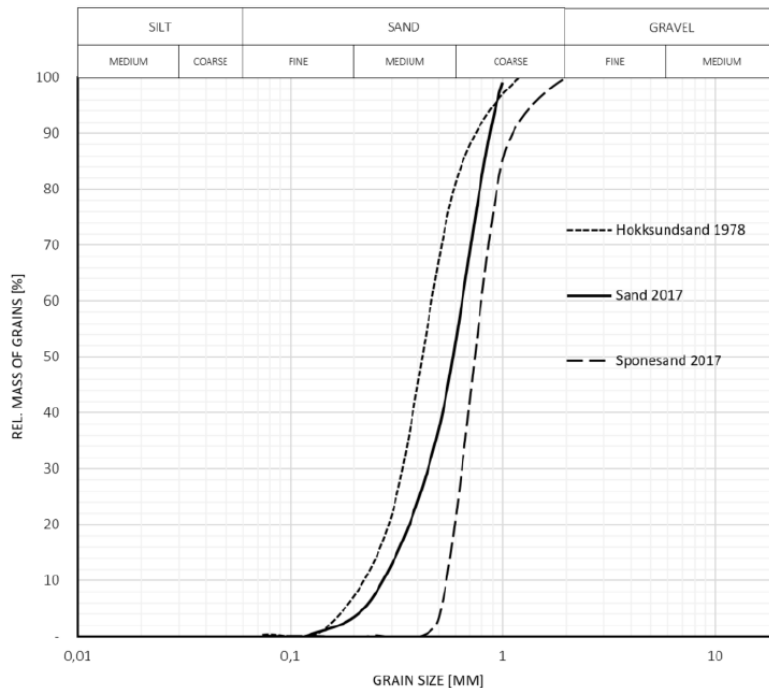


Figure 2.4: Grain size distribution

2.2.2 Grain density

The grain density of the material was found using a pycnometer and the standard-procedure found in ISO 17892-3:2004. The interpreted value was 2.64 g/cm^3 . (Søvik

2017)

2.2.3 Water content

The water content was found to be 0.007 %. (Søvik 2017)

2.2.4 Porosity limits and density

Using the procedures first described by DEGEBO the maximum porosity was approximated to $n_{max} = 46.4\%$ and the minimum dry density to 13.9 kN/m^3 . The lowest porosity was found by compacting the sand in a steel cylinder with four resulting layers of sand, each with a height of approximately 2 cm. (Søvik 2017) Each layer of saturated sand was compacted by vibration, caused by two rods hitting the exterior of the cylinder wall for 30 seconds, after which the excess surface water was removed. (Søvik 2017) The sample was then dried at what is considered its densest state and the minimum porosity found was $n_{min} = 35.4\%$ and maximum dry density 16.8 kN/m^3 . (Søvik 2017)

For calculating the density achieved in the testing chamber a cylindrical box with a known volume was placed in the test chamber and the chamber was then filled as usual. the dry weight of the sand could be measured then be calculated. The average in-situ density measured was $\gamma_{dry} = 15.75 \text{ kN/m}^3$ and the in-situ porosity is approximated to $n = 1 - \frac{\gamma_d}{\gamma_s} = 39\%$ which means that the relative density was around $D_r = 1 - \frac{n - n_{min}}{n_{max} - n_{min}} = 65\%$. (Søvik 2017) Therefore the sand is characterized as medium dense.

2.2.5 Triaxial tests

Some assumptions were made when interpreting the Triaxial tests. The oedometer stiffness is the same as the secant stiffness E_{50} , as no oedometer tests were done. (Søvik 2017) The cohesion is assumed negligible but is set to 0.1kPa to avoid numerical issues in Plaxis. (Søvik 2017) The dilatancy cut-off parameters are chosen on the basis of the contraction and dilative behavior observed in the triaxial tests. (Søvik 2017) The modulus exponent m was chosen by fitting a value corresponding with curves for both 20 and 30 kPa confining pressure.

The results of the most successful Triaxial tests are presented in Figure 2.7 and Figure 2.8.

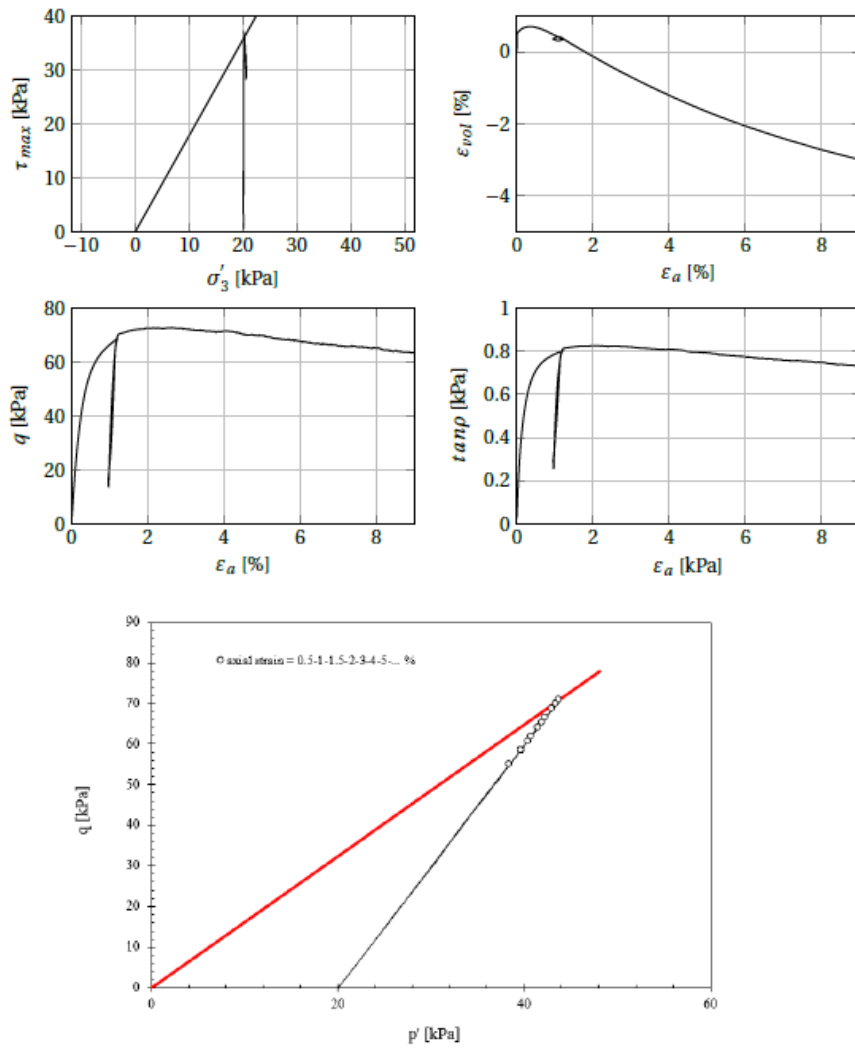


Figure 2.5: Triaxial test with a confining pressure of 20 kPa and relative density of 66.7% (Søvik 2017)

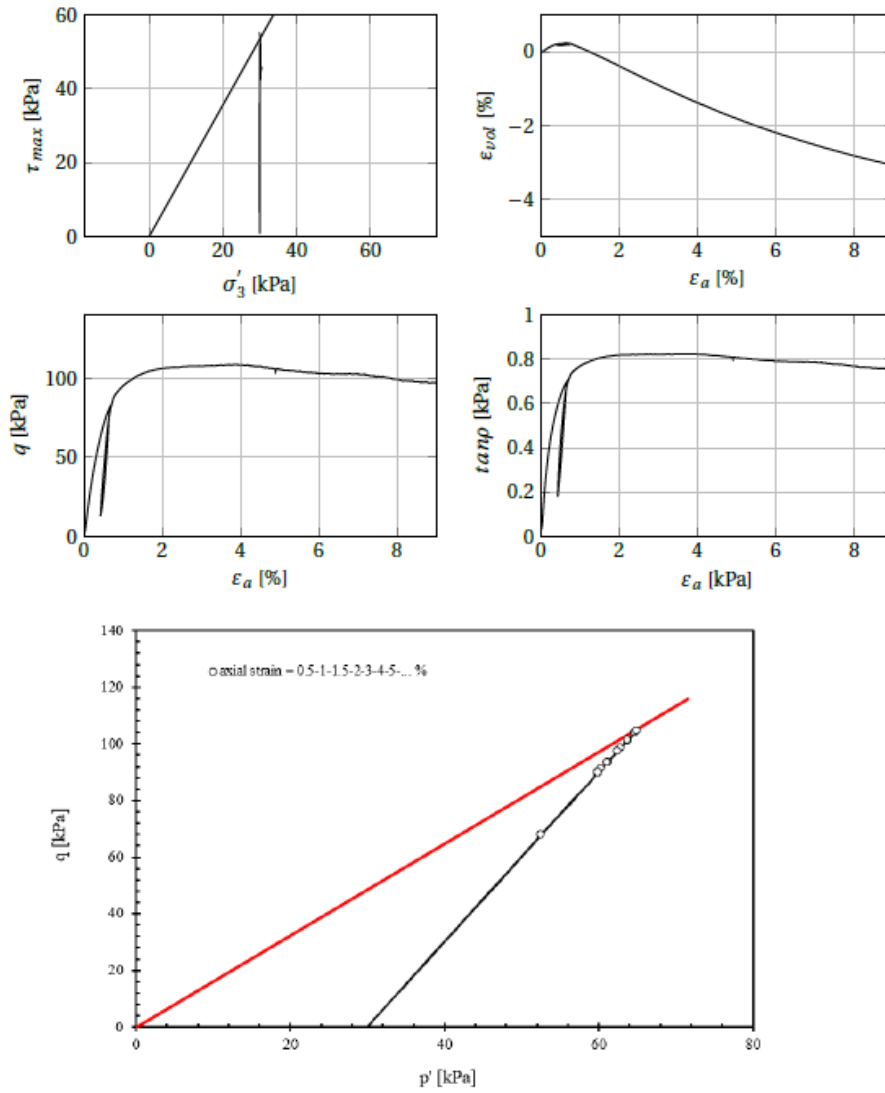


Figure 2.6: Triaxial test with a confining pressure of 30 kPa and relative density of 59.1% (Søvik 2017)

These triaxial tests were compared with one set of parameters in Soil-Test and is presented in Figure 2.7 and Figure 2.8. The associated Hardening Soil parameters are given in Table 2.2.

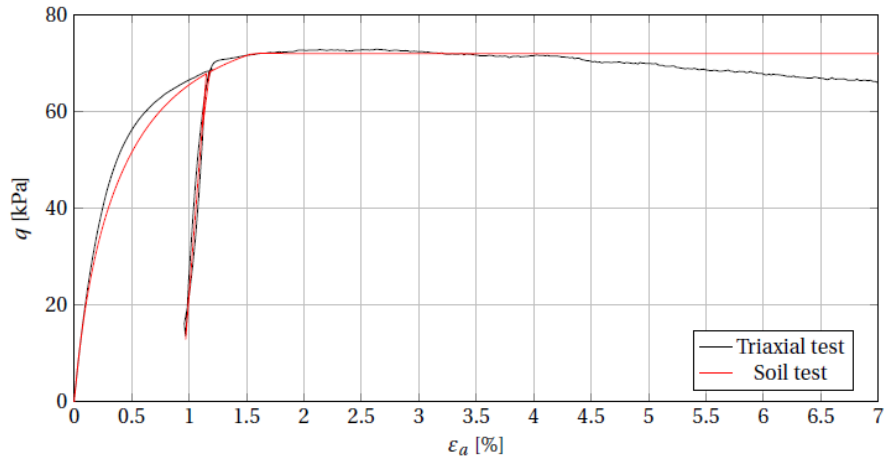


Figure 2.7: Triaxial- and Soil test with a relative density of 67% and confining pressure 20 kPa (Søvik 2017)

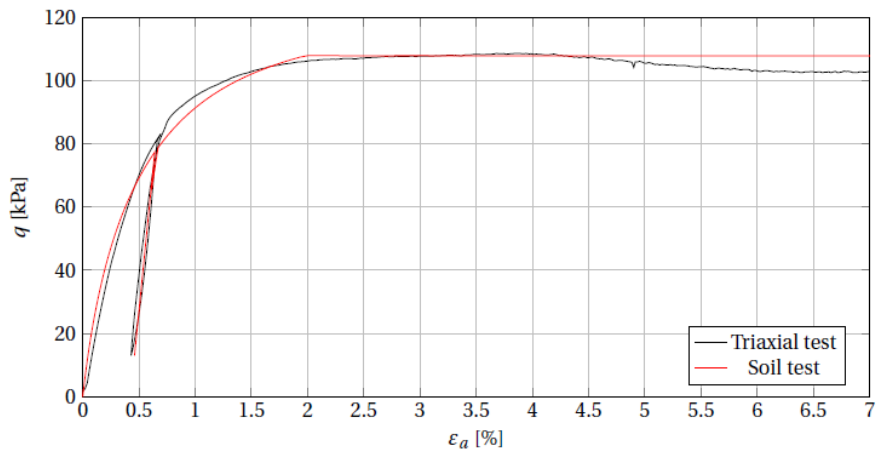


Figure 2.8: Triaxial- and Soil test with a relative density of 59% and confining pressure 30 kPa (Søvik 2017)

2.2.6 Summary of soil properties

Table 2.1: Index test summary. (Søvik 2017)

Parameters	Value
$C_u = \frac{d_{60}}{d_{10}}$	2.3
d_{50}	0.6 mm
ρ_s	2.64 g/cm ³
w	0
n_{max}	46.4%
n_{min}	35.4%
D_r	65%

Table 2.2: Hardening Soil parameters summary. (Søvik 2017)

Parameters	Value
E_{50}^{ref}	28 MPa
E_{oed}^{ref}	28 MPa
E_{ur}^{ref}	58 MPa
m	0.4
R_f	0.85
OCR	1
$K_0^{NC} = K_0$	$1 - \sin(\phi) = 0.36$
ϕ	39.5°
ψ	11.5°
c	0.1 kPa
v_{ur}	0.2
e_{init}	0.645
e_{max}	0.71
p_{ref}	100 kPa

2.3 Interpreting shear modulus G

The pressuremeter is an ideal test for measuring the shear modulus of the ground since the shear modulus is independent of drainage. (Clarke 1997) The shear modulus is interpreted from the unloading-reloading cycle performed using the pressuremeter, either from the loading phase, unloading phase or an average of the two, as shown in Figure 2.9. The inclination of the loop when plotting the pressure P [kPa] on the y-axis and $\epsilon_\theta = \frac{\Delta R}{R_0}$ on the x-axis will equal two times the shear modulus. (Clarke 1997)

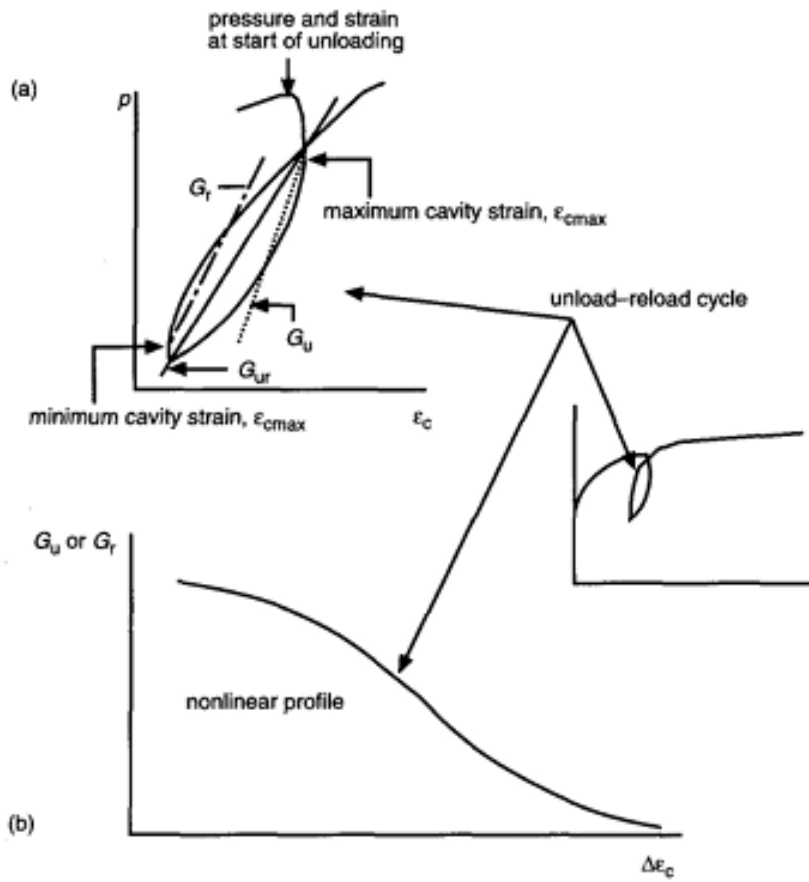


Figure 2.9: The selection of shear moduli from an unload-reload cycle showing (a) the unload and reload secant moduli and (b) the nonlinear profile. G_{ur} = secant modulus from whole cycle; G_u = secant unload modulus measured from maximum cavity strain; G_r = secant reload modulus measured from minimum cavity strain. (Clarke 1997)

Chapter 3

Testing procedure

3.1 Initial testing of the equipment

The first part of the testing was focused on determining the quality of the pressuremeter. The tests consisted of different ways of inflating the rubber ballow of the two pressuremeter. The purpose of the testing was to check how the rubber behaved under applying/releasing pressure. The Volumetric/radial changes were also investigated during applying/releasing pressure. Negative impacts would have been if the glue was not holding or if the change in size varied over the length of the rubber sleeve.

3.1.1 Materials, equipment, and test setup

The tests included:

1. Hand pump for increasing the pressure in the system
2. Electric pump to control the volume of water going into the system
3. Pressure Gauge
4. Ball Valve
5. Flow Control Valve
6. Pressure transmitter
7. Coupling
8. Pressuremeter with vulcanized rubber sleeve Shore 50
9. Pressuremeter with vulcanized rubber sleeve Shore 70

The setup used is shown in Figure 3.1.

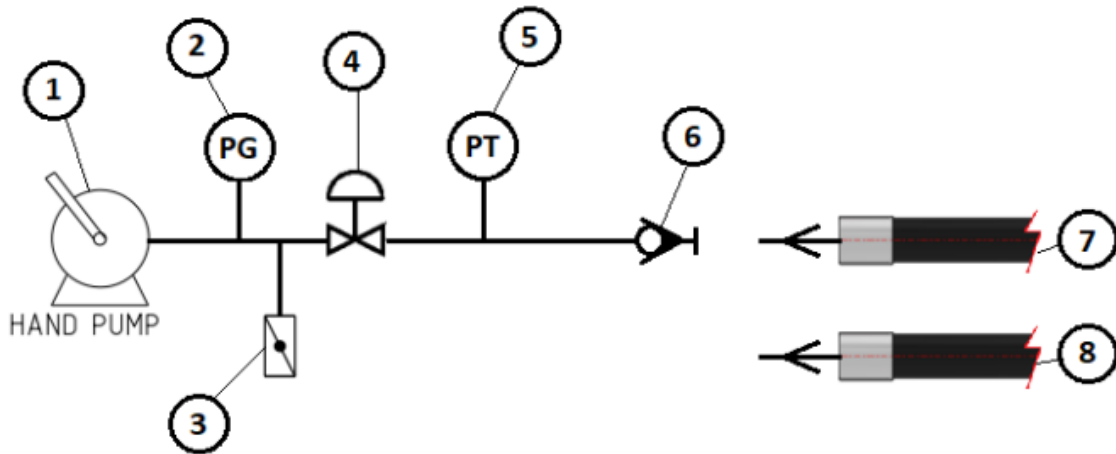


Figure 3.1: Setup schematic

3.1.2 Initial measurement before testing

Before starting all of the tests, the rubber sleeve (Shore 50, shore 70) was checked to record the reference readings for the test. The reference measurements included measuring the sleeve diameter at the measurement points along the length of the rubber sleeve (between 0-45 cm). The measurement points are marked in Figure 3.2.

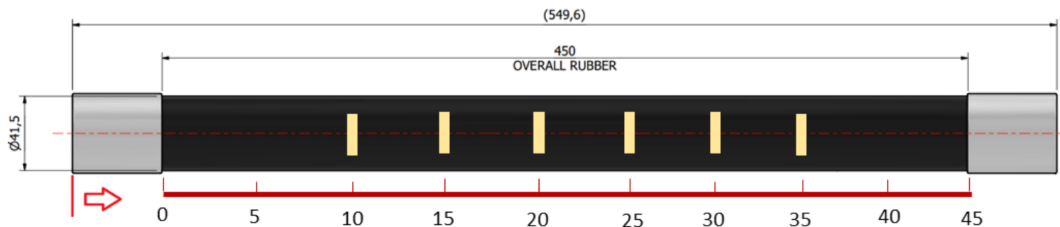


Figure 3.2: Measure points along the test tool

3.1.3 Removing the air and checking for leaks

The best solution to get the test setup containing the least amount of air at the start was to prefill the system. Test pieces 7 and 8 were placed vertically and filled up with water. The other part of the system was filled up by using the pump. First, the ball valve (3) was placed barely open and placed at the highest point. Then water was pumped until only water came out of the ball valve (3).

To check for leaks the system was pressurized to 10 % over the normal pressure for normal testing and held for 15 min. Pressure for normal testing varies for all tests.

3.1.4 Expansion test in the air; Stress-controlled

The expansion test with a continuous rate of pressure application in the air was performed to investigate the volumetric and radial strain under expanding and contracting the rubber bellow.

Procedure:

1. Measure the rubber sleeve diameter at defined points.
2. Prepare the test set-up and connect the test tool, and follow the procedure to remove the trapped air inside the tool.
3. Measure the rubber sleeve diameter at defined points again, and record if there were any changes in the measured diameters with the measurements at No. 1.
4. Start applying pressure to the test tool with the minimum rate possible with the pump. Check the rubber movement carefully and record the minimum pressure needed to make the rubber start moving. Continue with recording the flow to the test tool and measure the diameter at measurement points.
5. When reached to 50 % radial strain, stop applying pressure and start releasing the pressure with the same rate as used in No. 4. Record the flow out of the test tool and measure the diameter at measurement points.
6. After the test is finished, measure the diameter at measurement points and compare it with measurements at No. 1.
7. Perform the test for both test tools (shore 50 and shore 70).

3.1.5 Expansion test in the air; Strain-controlled

The volumetric strain-controlled test in the air was performed to evaluate the pressure changes in the test tool and associated radial strain.

Procedure:

1. Measure the rubber sleeve diameter at defined points
2. Prepare the test set-up, connect the tool, and follow the procedure to remove the trapped air inside the tool.
3. Measure the rubber sleeve diameter at defined points again, and record if there were any changes in the measured diameters with the measurements at No. 1.
4. Start injecting water at a constant rate. Record the pressure and measure the diameter at measurement points. The hand pump injects 16 ml in each stroke

5. When reached 50 % radial strain, stop injecting water and start releasing the water at the same rate as used in No. 4. Record the pressure and measure the diameter at measurement points.
6. After the test is finished, measure the diameter at measurement points and compare it with measurements at No. 1.
7. Perform the test for both test tools (shore 50 and shore 70).

3.1.6 Expansion test in the air; Strain-controlled with unload-reload loops

The volumetric strain-controlled test in the air, with three unload-reload loops, will be performed to evaluate the pressure changes in the test tool and associated radial strain.

Procedure:

1. Measure the rubber sleeve diameter at defined points
2. Prepare the test set-up, connect the tool, and follow the procedure to remove the trapped air inside the tool.
3. Measure the rubber sleeve diameter at defined points again, and record if there were any changes in the measured diameters with the measurements at No. 1.
4. Start injecting water at a constant rate. Record the pressure and measure the diameter at measurement points. The hand pump injects 16 ml in each stroke
5. When reached 10 % radial strain, stop injecting water and start releasing the water with the same rate as used in No. 4 until reaching 5 % radial strain. Record the pressure and measure the diameter at measurement points.
6. When reaching 5 % radial strain, start injecting water again (with the same rate as used in No. 4) until reaching 20 % radial strain. Record the pressure and measure the diameter at measurement points
7. When reached 20 % radial strain, stop injecting water and start releasing the water at the same rate as used in No. 4 until reaching 15 % radial strain. Record the pressure and measure the diameter at measurement points.
8. When reached 15 % radial strain, start injecting water again and with the same rate as used in No. 4 until reaching 50 % radial strain. Record the pressure and measure the diameter at measurement points.
9. When reached 50 % radial strain, stop injecting water and start releasing the water at the same rate as used in No. 4. Record the pressure and measure the diameter at measurement points.

10. After the test is finished, measure the diameter at measurement points and compare it with measurements at No. 1.
11. Perform the test for both test tools (shore 50 and shore 70).

An example of an expansion test; Strain-controlled with unload-reload loops is shown in Figure 3.3.

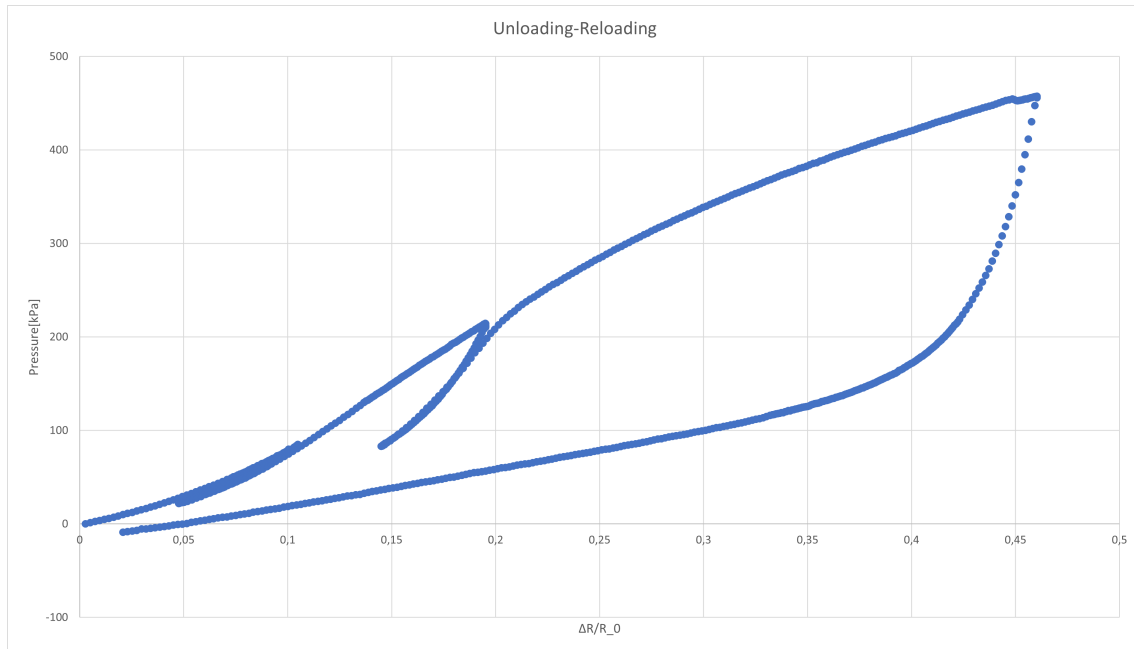


Figure 3.3: Example of applied pressure vs radial strain in a pressuremeter test

3.1.7 Expansion test in soil; Stress-controlled

The expansion test with a continuous rate of pressure application placed in a selected bed of soil will be performed to investigate the changes in the volume under expanding and contracting the rubber bellow.

Procedure:

1. Measure the rubber sleeve diameter at defined points
2. Prepare the test set-up, connect the tool, and follow the procedure to remove the trapped air inside the tool.
3. Start applying pressure to the test tool with the minimum rate possible with the pump. Continue with recording the flow to the test tool. For each step of pressure increase, the same duration should be used as for a similar test in the air (Section Section 4.1.1).
4. When reaching the max pressure recorded at 50 % radial strain for the test in the air (Section Section 4.1.1), stop applying pressure and start releasing the

pressure with the same rate as used in No. 3. Record the flow out of the test tool.

5. After the test is finished, take the test tool carefully out of the soil and measure the diameter at measurement points.
6. Perform the test for both test tools (shore 50 and shore 70).

3.1.8 Expansion test in the soil; Strain-controlled

The volumetric strain-controlled test in the air was performed to evaluate the pressure changes in the test tool and associated radial strain.

Procedure:

1. Measure the rubber sleeve diameter at defined points
2. Prepare the test set-up, connect the tool, and follow the procedure to remove the trapped air inside the tool.
3. Start injecting water at a constant rate and record the pressure. For each step of volume increase, the same duration should be used as for a similar test in the air (Section 4.1.2).
4. . When reaching the max volume recorded at 50 % radial strain for the test in the air (Section 4.1.2), stop injecting water and start releasing the water at the same rate as used in No. 3. Record the pressure.
5. After the test is finished, take the test tool carefully out of the soil and measure the diameter at measurement points
6. Perform the test for both test tools (shore 50 and shore 70).

3.2 Pressuremeter test in sand in large chamber

3.2.1 Materials, equipment, and test setup

The tests did include:

1. Computer controlled pump for controlling the amount of water injected into the system and measuring the pressure
2. Flow Control Valve
3. Coupling
4. Test piece with vulcanized rubber sleeve Shore 70

3.2.2 Procedure

For the tests in the large chamber, the pressuremeter was placed at a depth of 1.2 m in the center of the chamber. That gave a distance of 200cm from each wall and the chamber was filled with sand to a depth of 1m to the midpoint of the pressuremeter. The chamber was filled with sand according to the process previously described, and it took about 3 hours.

The pressure meter was connected to a pump that measured both the system's pressure and the injected water once every second. The pump was controlled by a program, shown in Figure 3.4, where the amount of injected water could be controlled. The tests were run at a rate of 2-4 ml/s, using the constant flow option in the program.

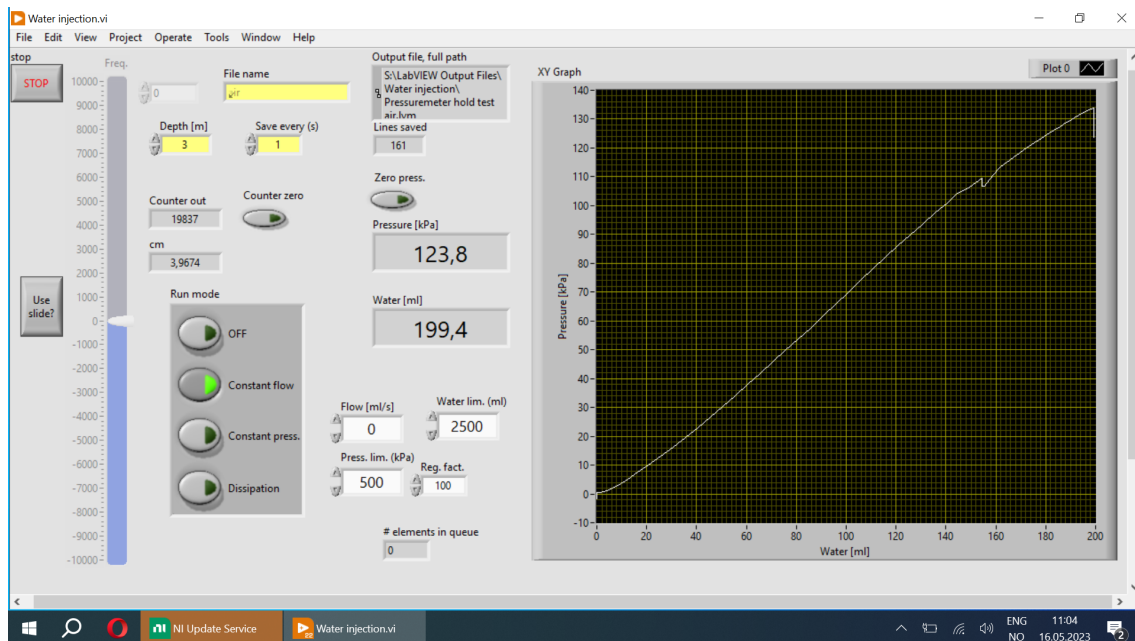


Figure 3.4: Screenshot of the program used to control the pump and log the results of the pressuremeter test

The loops were performed at 10% and 20% increase in radius and for each of the loops decreased 5% and then increased again. The test was continued until a 50% increase in radius and unloaded back down to the original state. The amount of water injected to reach those increases in radius was calculated based on the initial tests when performing unloading-reloading loops in air. The amount of water injected and the diameter at those points is shown in Table 3.1 and Table 3.2. The test in soil was performed 4 times in the same borehole. For two of the tests, there was performed an extra loop at an injected volume of 350 ml down to 300 ml to see if it made any changes to the shear modulus.

Table 3.1: Volumes changes calculated from diameter measurements of unloading reloading loops in the initial tests

Points	At 10% Strain	At 5% Strain	At 20% Strain	At 15% Strain	At 50% Strain
5	96.48 ml	42.80 ml	188.54 ml	136.60 ml	497.34 ml

Table 3.2: Measurements of the diameter [mm] at different strain levels during the initial tests

Points	Initial	After Bleeding	10% Strain	5% Strain
5	40.82	40.6	40.92	40.65
10	41.32	41.2	45.37	42.94
15	41.28	41.09	45.52	42.99
20	41.39	40.8	45.54	43.14
25	40.83	41.17	45.66	43.01
30	41.41	41.13	45.76	43.29
35	41.46	40.78	45.47	43.2
40	41.27	40.9	43.12	41.98
Points	At 20% Strain	At 15% Strain	At 50% Strain	After Pressure
5	41.6	41.31	41.56	40.68
10	49.27	47.08	60.89	41.59
15	49.52	47.28	60.87	42.35
20	49.84	47.28	60.85	42.2
25	49.32	47.61	61.76	42.55
30	49.85	47.65	61.56	42.35
35	49.4	47.2	60.78	41.42
40	44.16	43.21	47.92	41.28

3.3 Pressuremeter test in air with Unloading-reloading loops

The pressuremeter is made of an elastic rubber held together at both ends of the pressuremeter. This means that even as the pressuremeter expands in air, without any force from the soil, it requires an increased pressure. That pressure needed to be subtracted from the Unloading-reloading curves of the tests done in sand, to figure out the stiffness of the sand itself. The procedure of the test in air was exactly the same as for the tests in sand.

3.4 Simulating the pressuremeter test in Plaxis 2D

PLAXIS 2D is a powerful and user-friendly finite-element (FE) software for 2D analysis of deformation and stability in geotechnical engineering and rock mechanics. (*Plaxis 2D 2023*) Also, PLAXIS 2D is ideal for a range of applications from excavations, embankments, and foundations to tunneling, mining, oil and gas, and reservoir geomechanics. (*Plaxis 2D 2023*) It includes all the essentials to perform deformation and safety analysis for soil and rock that do not require the consideration of creep, steady state groundwater or thermal flow, consolidation analysis, or any time-dependent effects. (*Plaxis 2D 2023*)

Plaxis was used to simulate the pressuremeter test as a perfect cylinder expanding in the soil. The soil is modeled to represent to the one used in the chamber tests. The plaxis simulation was based on an axisymmetric model in which you draw the model as a slice of a cylinder and then this slice is rotated around the left boundary, as shown in Figure 3.5

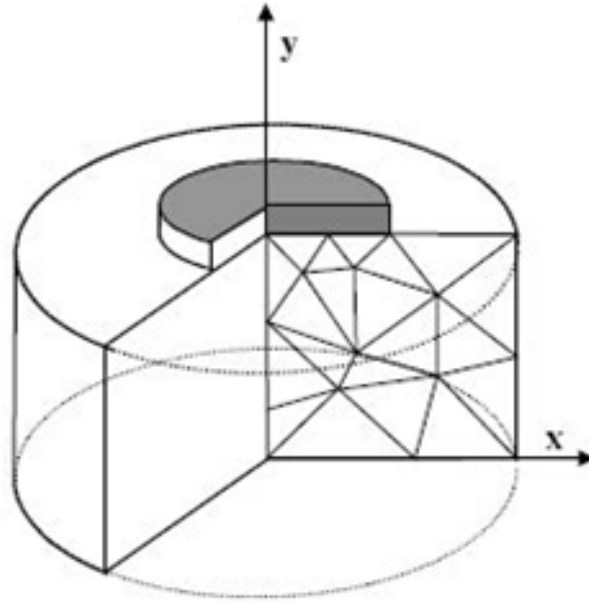


Figure 3.5: Model of how the axisymmetric model works in Plaxis2D (*Plaxis 2D* 2023)

The soil in the model used the Hardening soil model, which is an advanced model for the simulation of soil behavior. The Hardening soil model is based on the Mohr-Coulomb model, which describes the soil by friction angle ϕ , the cohesion c , and the dilatancy angle ψ . (*Plaxis 2D* 2023) The difference is that the hardening soil model describes the soil much more accurately by using three different input stiffnesses: the triaxial stiffness E_{50} , the triaxial unloading stiffness E_{ur} and the oedometer loading stiffness E_{oed} . (*Plaxis 2D* 2023) It also accounts for the stress-dependency of stiffness moduli, which means that all stiffnesses increase with pressure based on a reference stress of 100 kPa (1 Bar). (*Plaxis 2D* 2023) All the input parameters that were put into the soil model are shown in Table 2.2.

The pressuremeter was modeled as a perfect cylinder with a radius of 20 mm and a height of 350 mm. The wall of the cylinder was then expanded until it hit 50% strain and then back to the original state. It was supposed to be modeled to do the same loops as the pressuremeter test in soil, but after unloading the force on the pressuremeter returned to zero. That meant that the sand was able to stand by itself and not move together with the pressuremeter. This was the case for the loops at 10% and 20%, but at 50% it was possible to get a measurement of the unloading shear stiffness. The model of the pressuremeter simulated in Plaxis is shown in Figure 3.6.

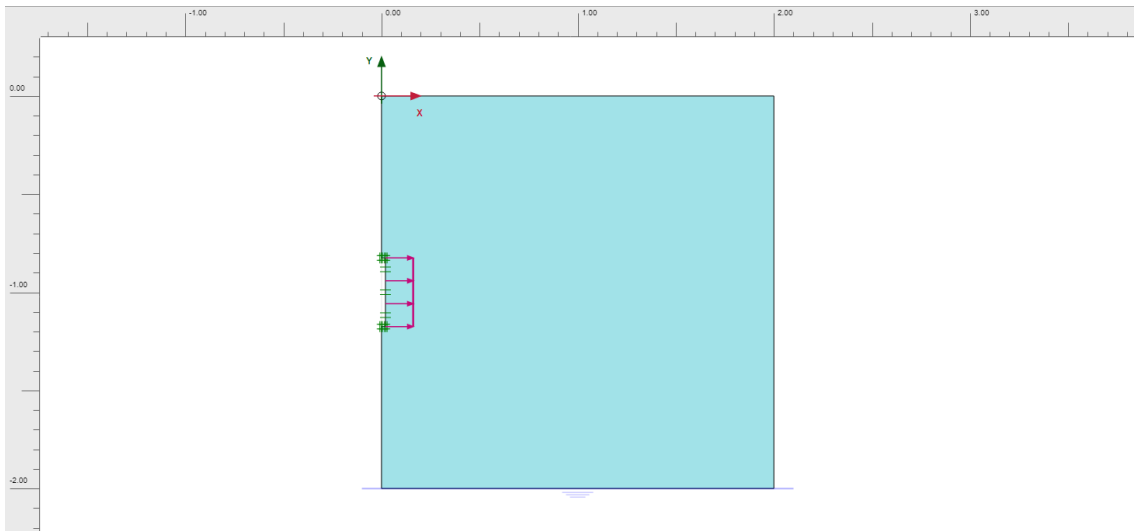


Figure 3.6: Model of pressuremeter in Plaxis2D

Chapter 4

Results

4.1 Results from initial tests

The purpose of the initial tests was to check the quality of the pressuremeter's material and confirm that it deformed uniformly.

4.1.1 Expansion test in the air; Stress-controlled

The test was performed according to the procedure and generated the change in diameter as shown in Figure 4.1 and Figure 4.3 and pressure as shown in Figure 4.2 and Figure 4.4. The results did not deviate from the expected values as some variation will occur when measuring manually.

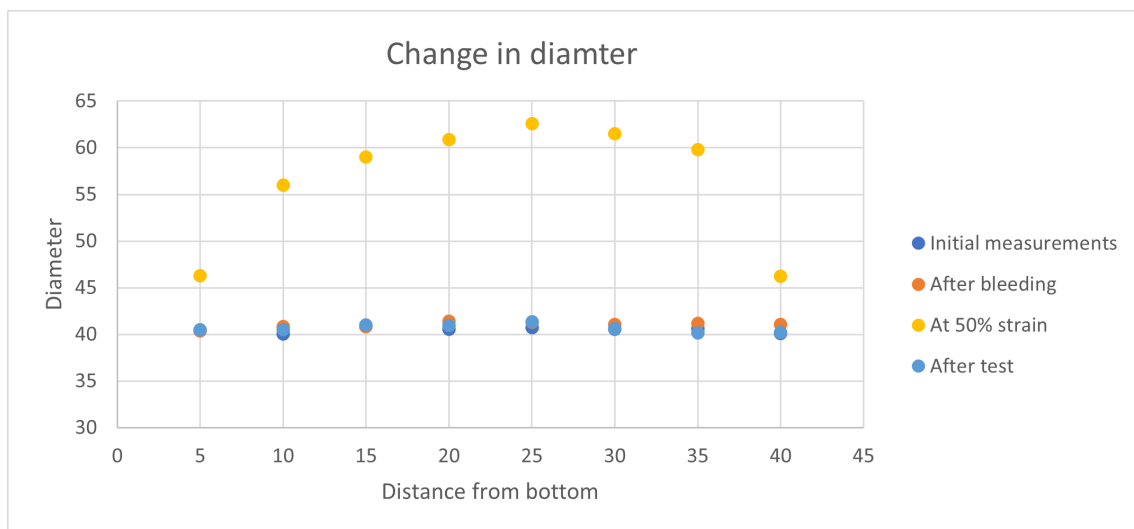


Figure 4.1: Change in the diameter of the rubber bellow, Shore 50, during test 7.2

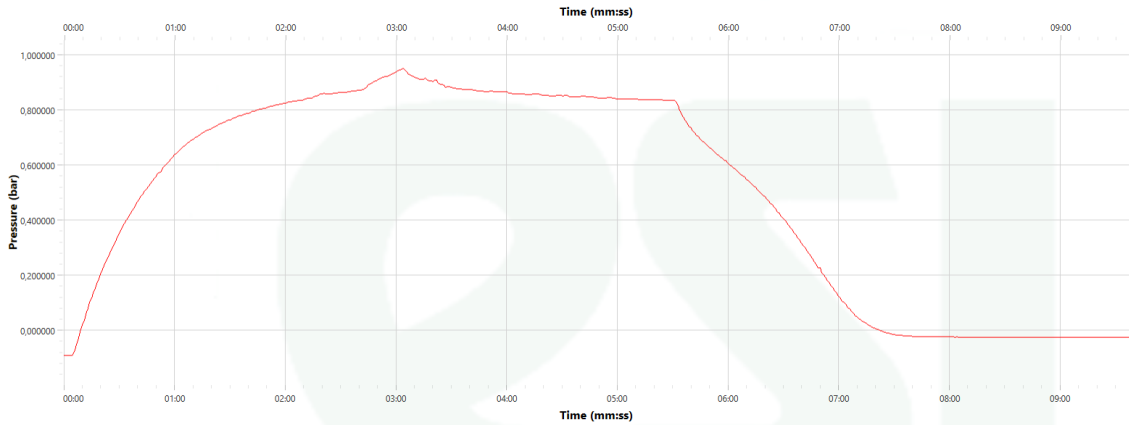


Figure 4.2: Change in pressure inside the rubber bellow, Shore 50, during test 7.2

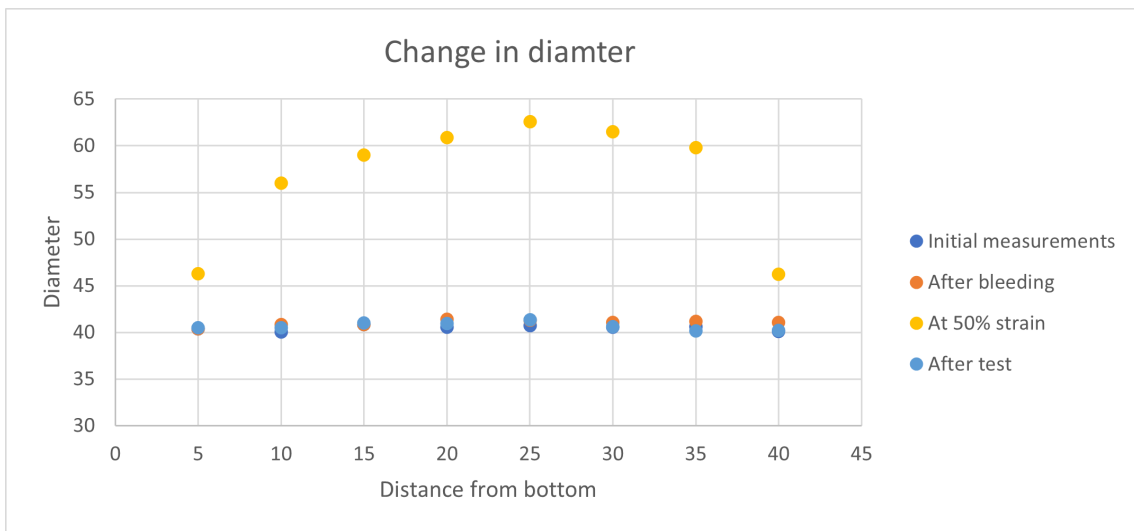


Figure 4.3: Change in the diameter of the rubber bellow, Shore 70, during test 7.2

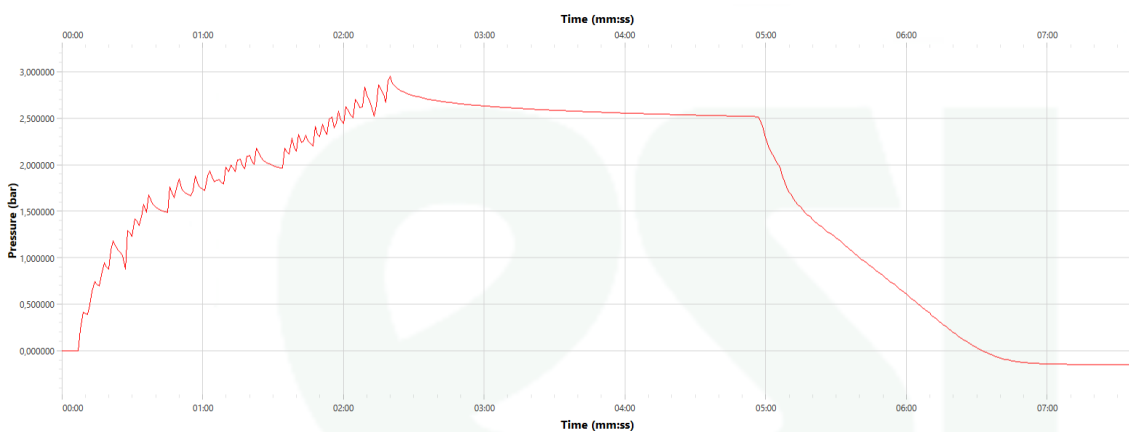


Figure 4.4: Change in pressure inside the rubber bellow, Shore 70, during test 7.2

4.1.2 Expansion test in the air; Strain-controlled

The test was performed according to the procedure and generated the change in diameter as shown in Figure 4.5 and Figure 4.7 and pressure as shown in Figure 4.6 and Figure 4.8 The results did not deviate from the expected values as some variation will occur when measuring manually.

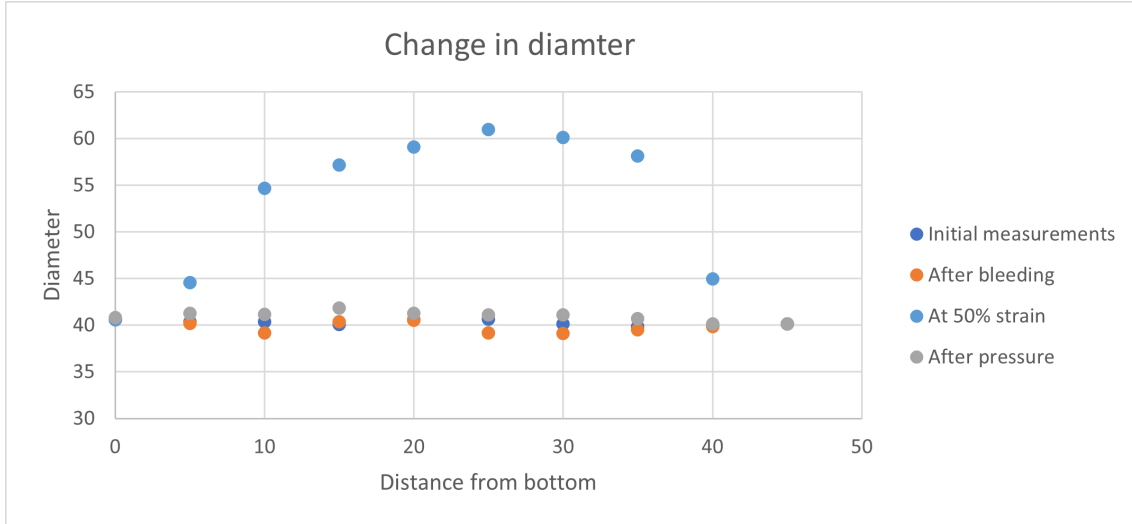


Figure 4.5: Change in the diameter of the rubber bellow, Shore 50, during test 7.3

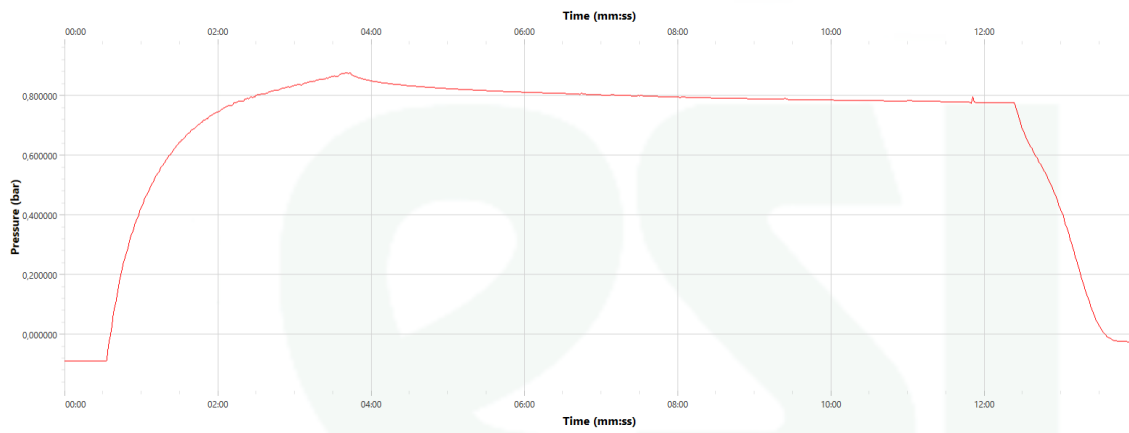


Figure 4.6: Change in pressure inside the rubber bellow, Shore 50, during test 7.3

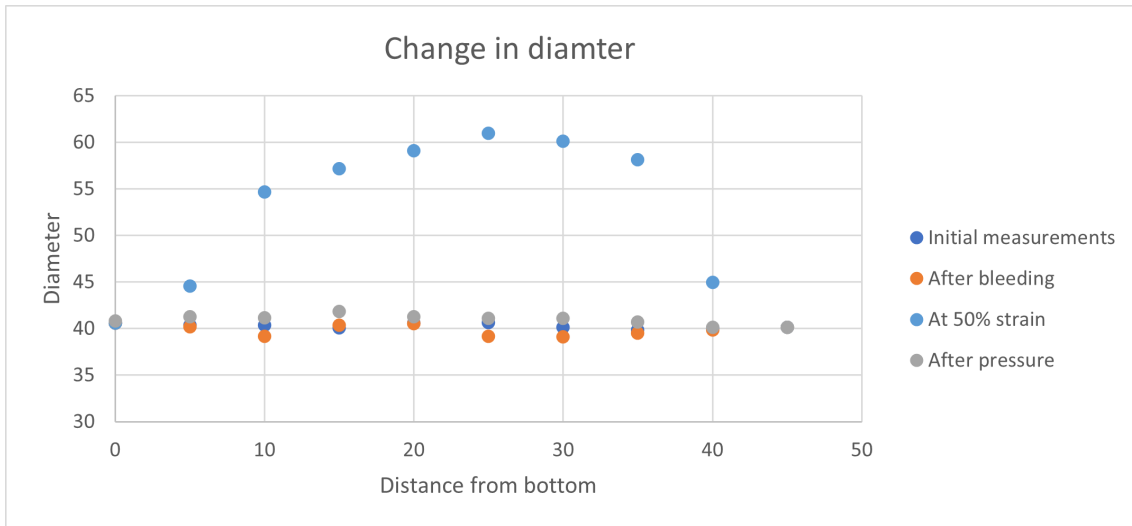


Figure 4.7: Change in the diameter of the rubber bellow, Shore 70, during test 7.3

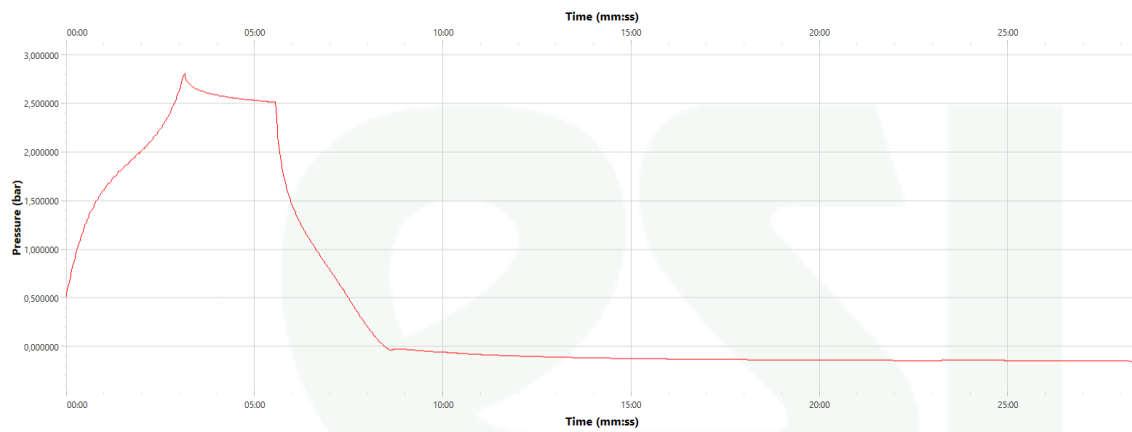


Figure 4.8: Change in pressure inside the rubber bellow, Shore 70, during test 7.3

4.1.3 Expansion test in the air; Strain-controlled with unload-reload loops

The test was performed according to the procedure and generated the change in diameter as shown in Figure 4.9 and Figure 4.11 and pressure as shown in Figure 4.10 and Figure 4.12. The results did not deviate from the expected values as some variation will occur when measuring manually.

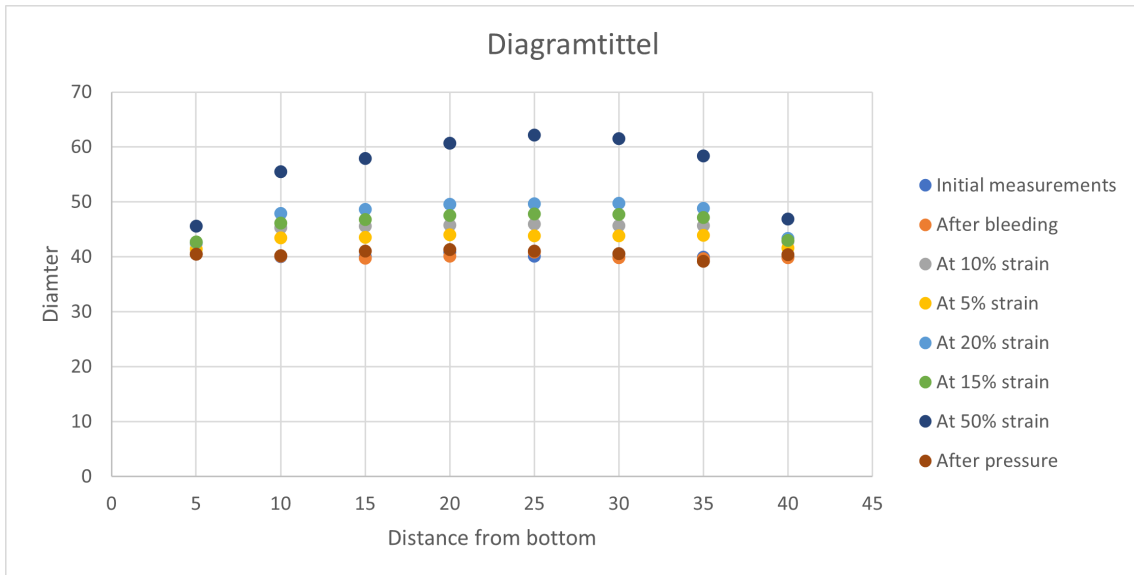


Figure 4.9: Change in the diameter of the rubber bellow, Shore 50, during test 7.4

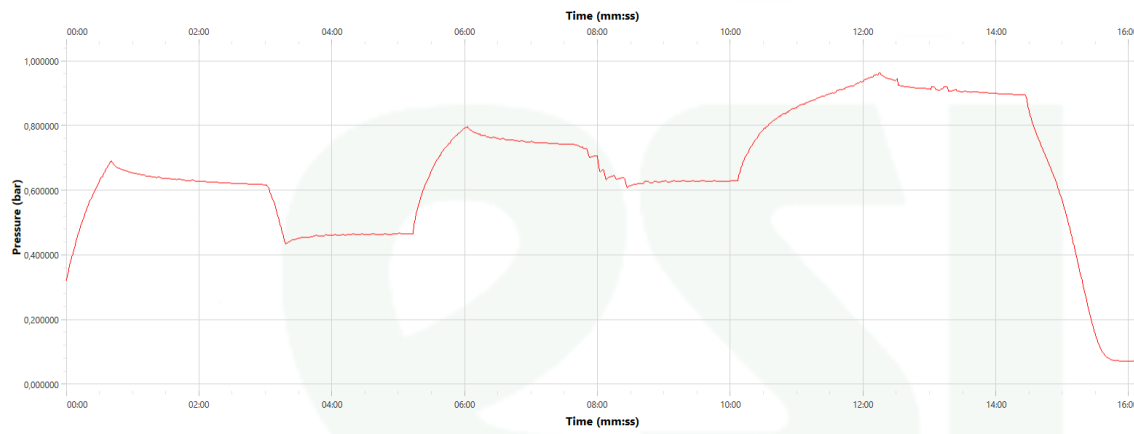


Figure 4.10: Change in pressure inside the rubber bellow, Shore 50, during test 7.4

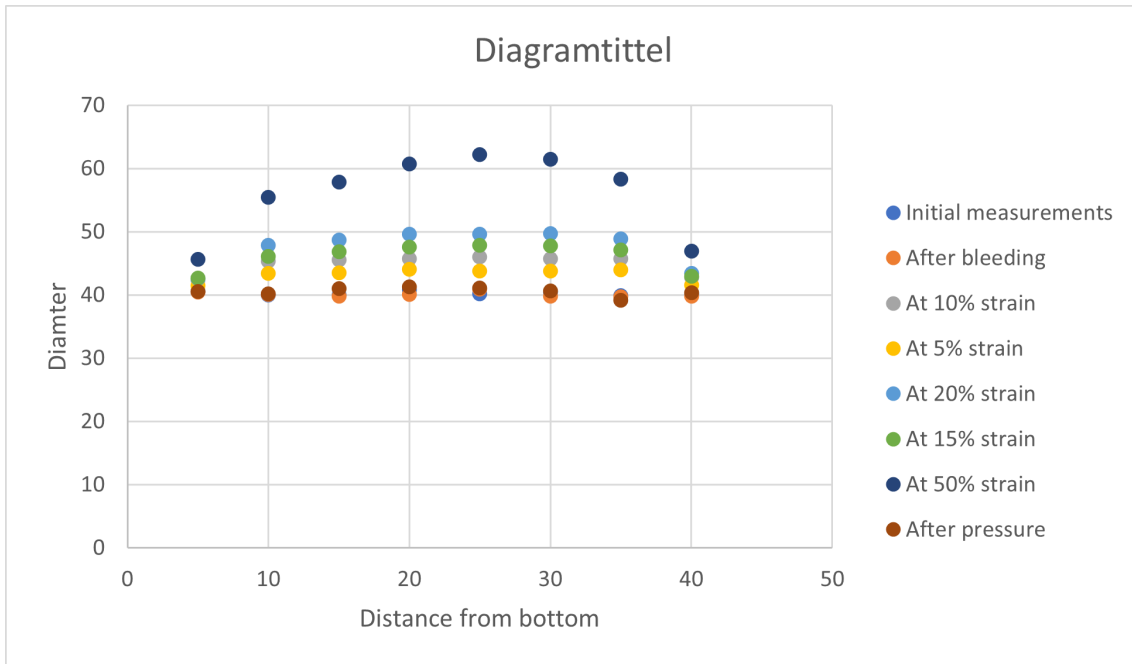


Figure 4.11: Change in the diameter of the rubber bellow, Shore 70, during test 7.4

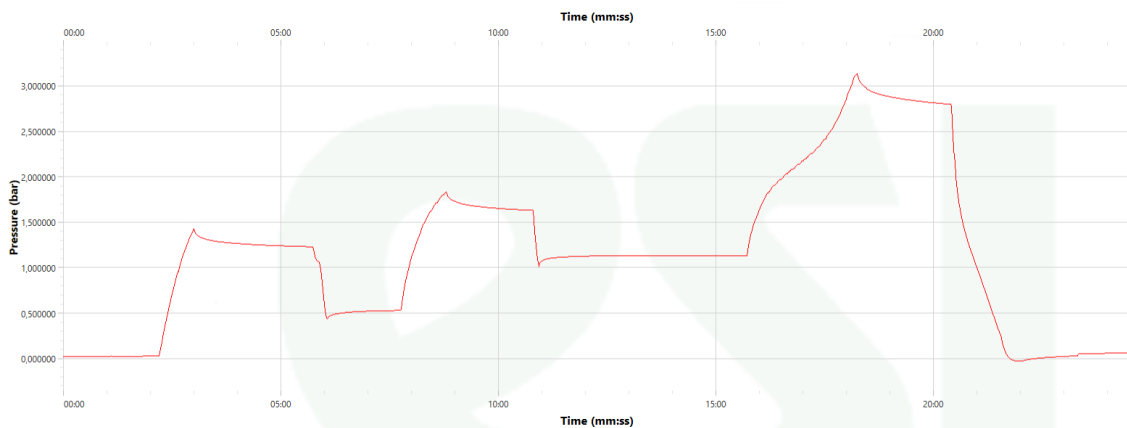


Figure 4.12: Change in pressure inside the rubber bellow, Shore 70, during test 7.4

4.1.4 Expansion test in soil; Stress-controlled

The test was performed according to the procedure and generated the change in diameter as shown in Figure 4.13 and Figure 4.15 and pressure as shown in Figure 4.14 and Figure 4.16. The slight deviation occurring in these results was most likely a result of the angle at which the pressuremeter was held not being vertical enough when measured after pressure creating a slightly elevated value.

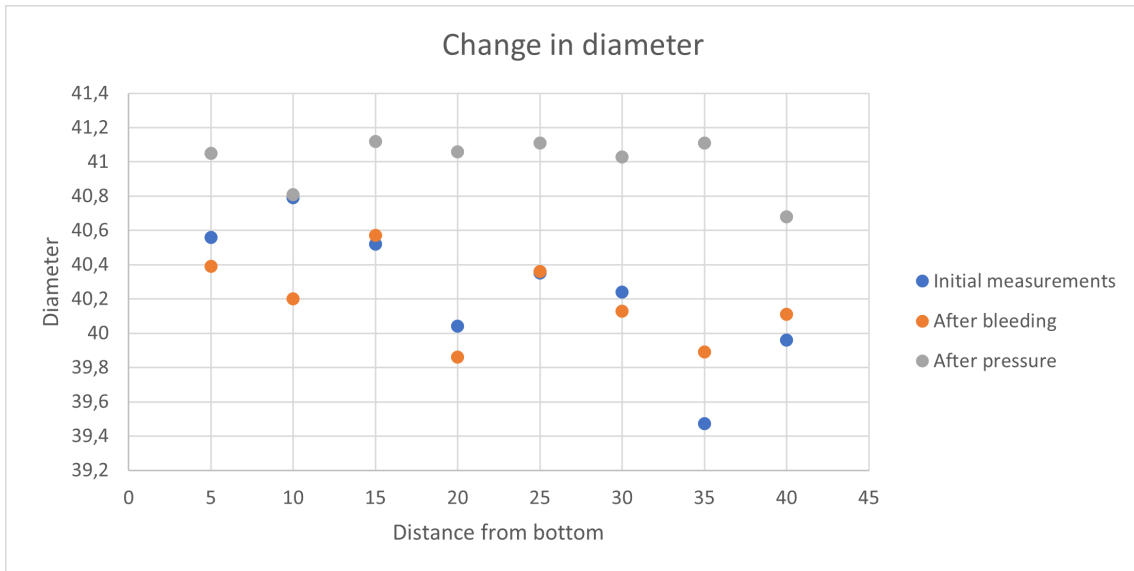


Figure 4.13: Change in the diameter of the rubber bellow, Shore 50, during test 7.5

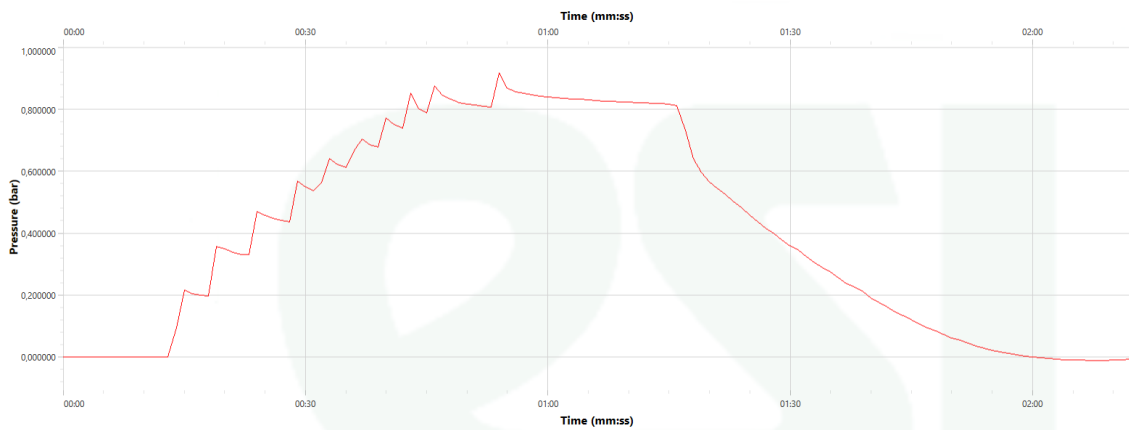


Figure 4.14: Change in pressure inside the rubber bellow, Shore 50, during test 7.5

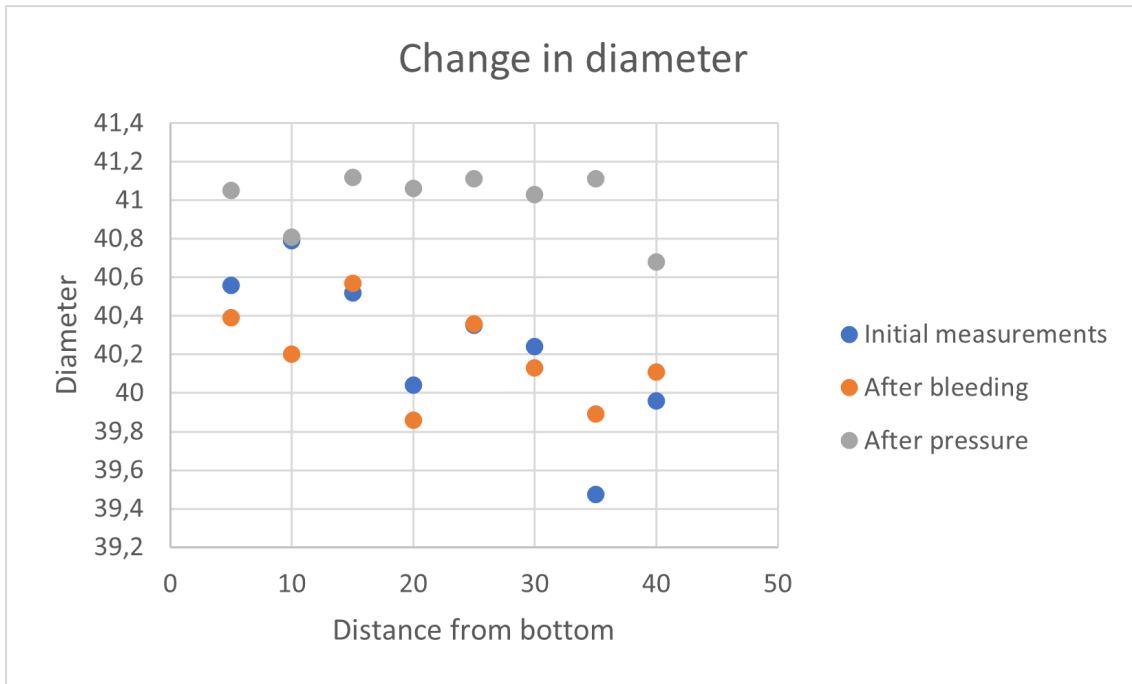


Figure 4.15: Change in the diameter of the rubber bellow, Shore 70, during test 7.5



Figure 4.16: Change in pressure inside the rubber bellow, Shore 70, during test 7.5

4.1.5 Expansion test in the soil; Strain-controlled

The test was performed according to the procedure and generated the change in diameter as shown in Figure 4.17 and Figure 4.19 and pressure as shown in Figure 4.18 and Figure 4.20. The results did not deviate from the expected values as some variation will occur when measuring manually. Especially in the case of measuring the diameter of the pressuremeter after it had been underground, there were problems with getting it to stay at the same angle as before.

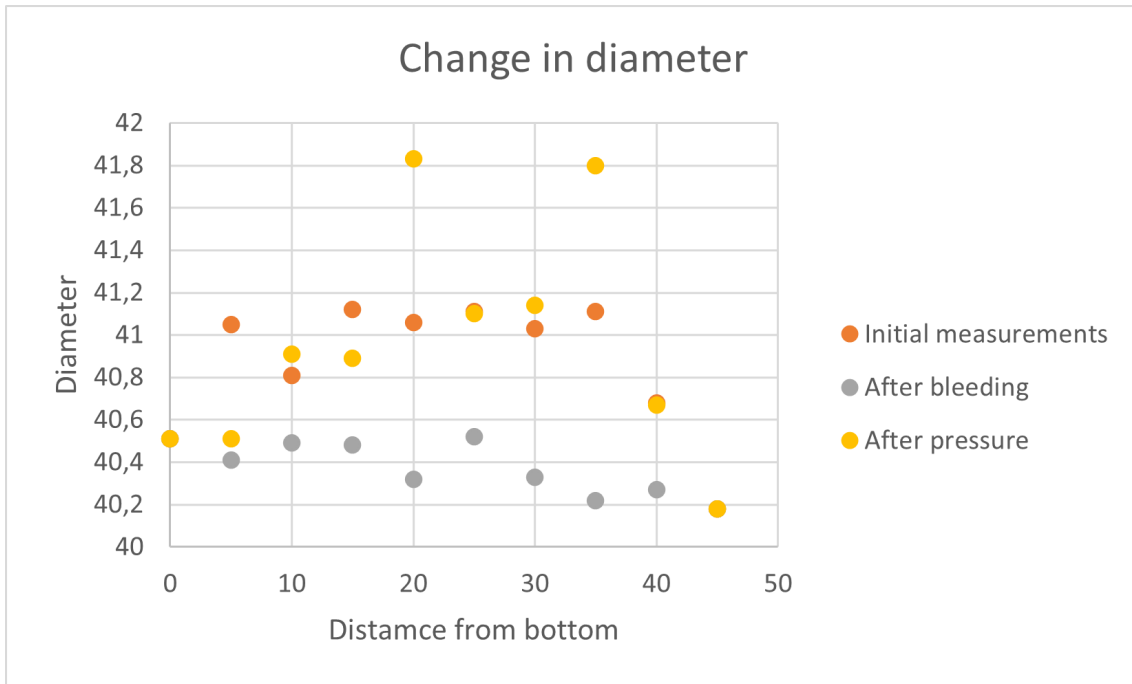


Figure 4.17: Change in the diameter of the rubber bellow, Shore 50, during test 7.6

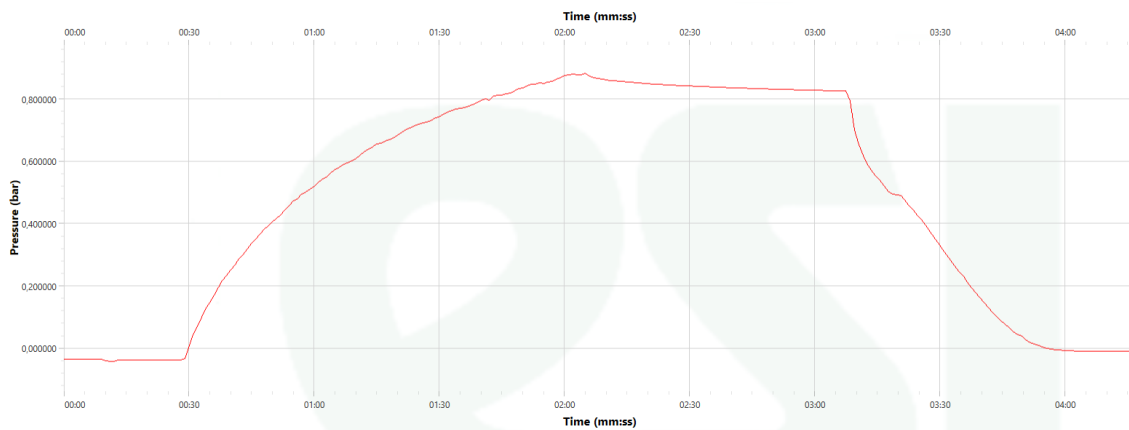


Figure 4.18: Change in pressure inside the rubber bellow, Shore 50, during test 7.6

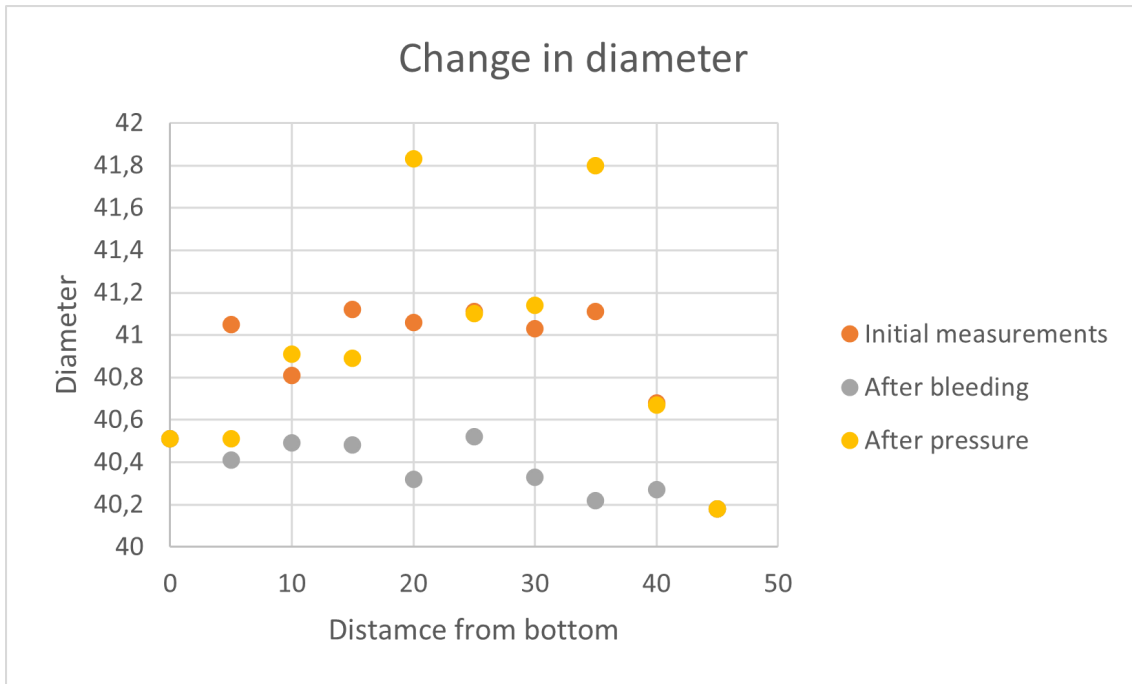


Figure 4.19: Change in the diameter of the rubber bellow, Shore 70, during test 7.6

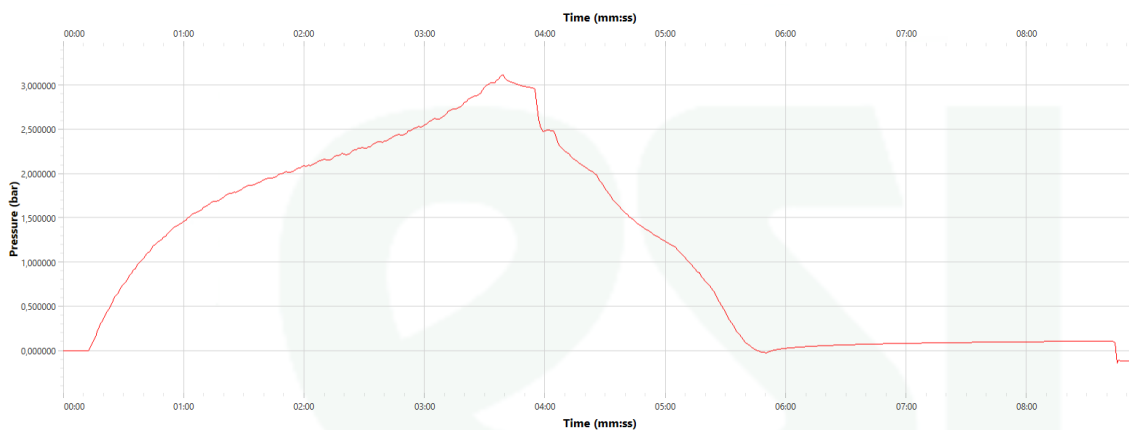


Figure 4.20: Change in pressure inside the rubber bellow, Shore 70, during test 7.6

4.2 Pressuremeter test in large chamber

The purpose of the large-scale tests, as explained before, was to figure out if this prototype of the pressuremeter could be used to find the shear modulus of the sand. The tests were performed 4 times in the soil and 2 times in air. The shear modulus, G_{Uncorr} , was the inclination of the unloading reloading loop taken directly from the test data. The stiffness, G_{ur} , was the stiffness of the sand corrected for the stiffness of the pressuremeter interpreted from the tests in air.

4.2.1 Unloading-Reloading stiffness

The plot of pressure vs. strain in Figure 4.21, Figure 4.22, Figure 4.23, and Figure 4.24 is the direct result of the four pressuremeter tests in soil. The uncorrected shear modulus G_{Uncorr} was calculated from the inclination of the unloading-reloading loops of the graphs and is presented in Table 4.1.

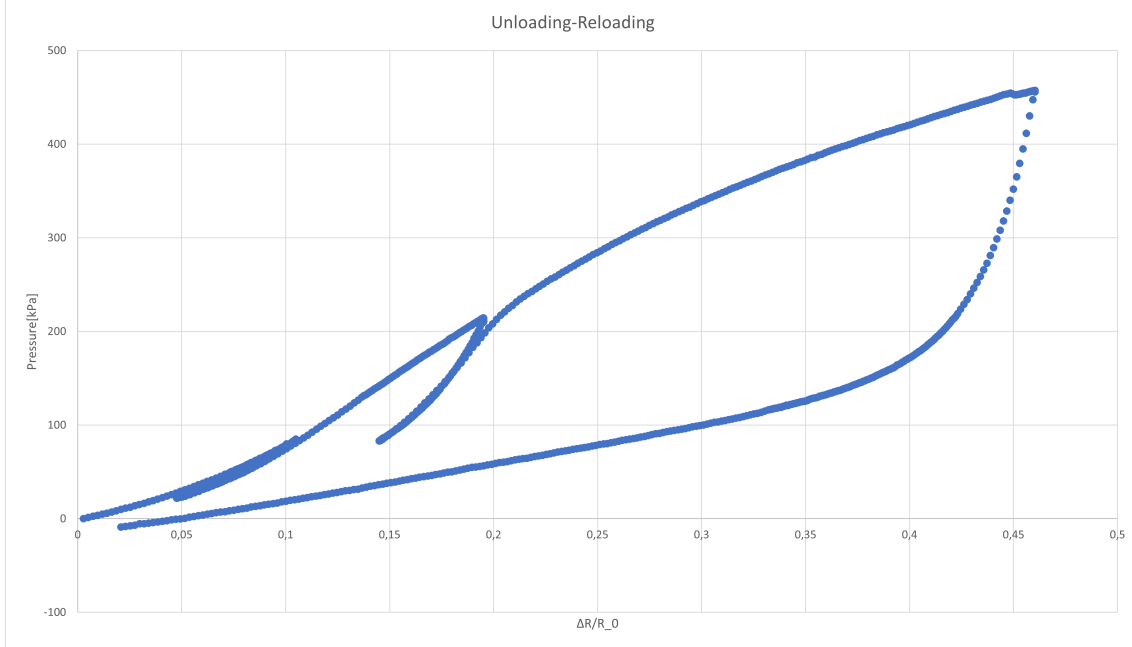


Figure 4.21: Plot of unloading reloading loops test 1, on the y-axis the pressure P [kPa] inside the pressuremeter and on the x-axis $\epsilon_\theta = \frac{\Delta R}{R_0}$

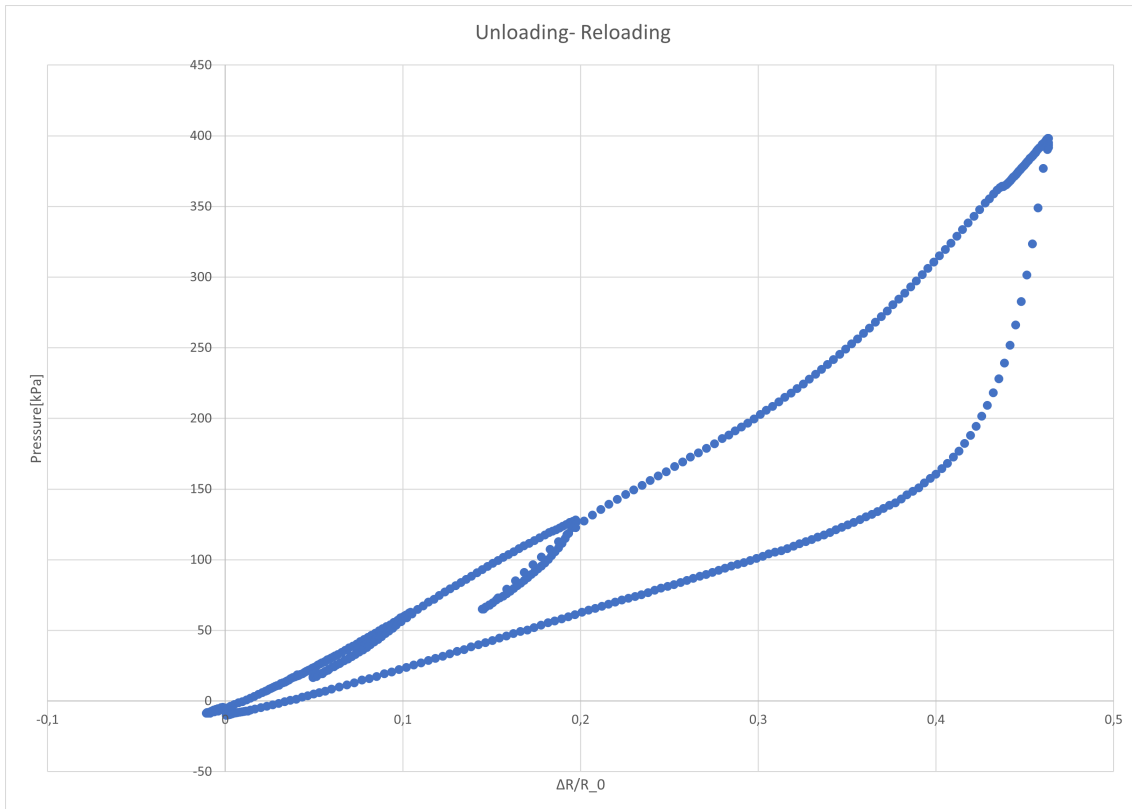


Figure 4.22: Plot of unloading reloading loops test 2, on the y-axis the pressure P [kPa] inside the pressuremeter and on the x-axis $\epsilon_\theta = \frac{\Delta R}{R_0}$

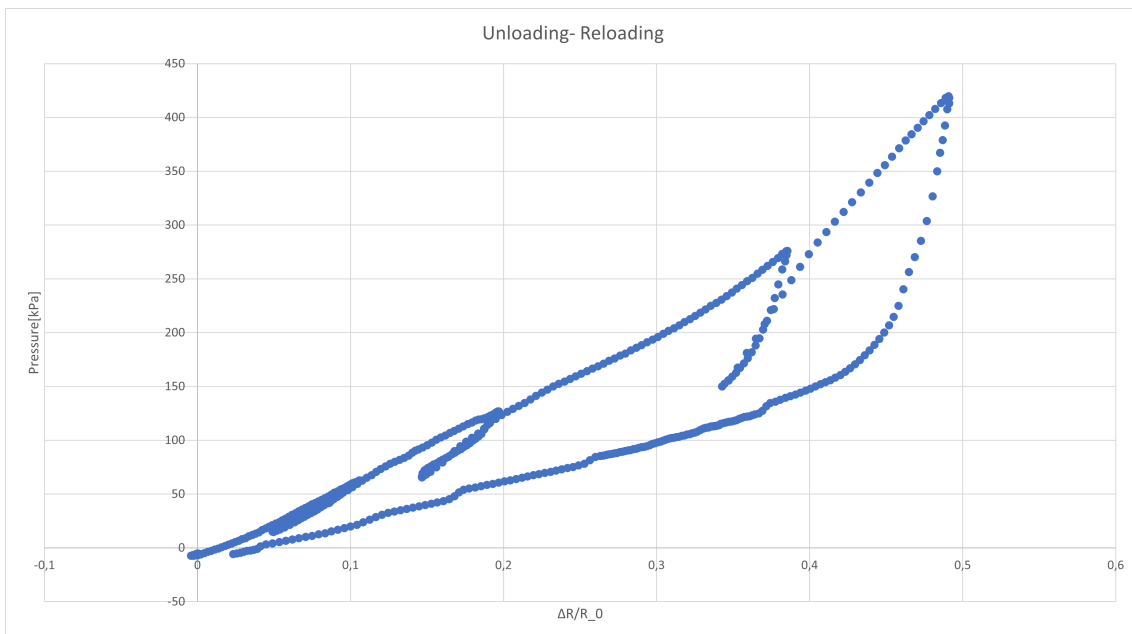


Figure 4.23: Plot of unloading reloading loops test 3, on the y-axis the pressure P [kPa] inside the pressuremeter and on the x-axis $\epsilon_\theta = \frac{\Delta R}{R_0}$

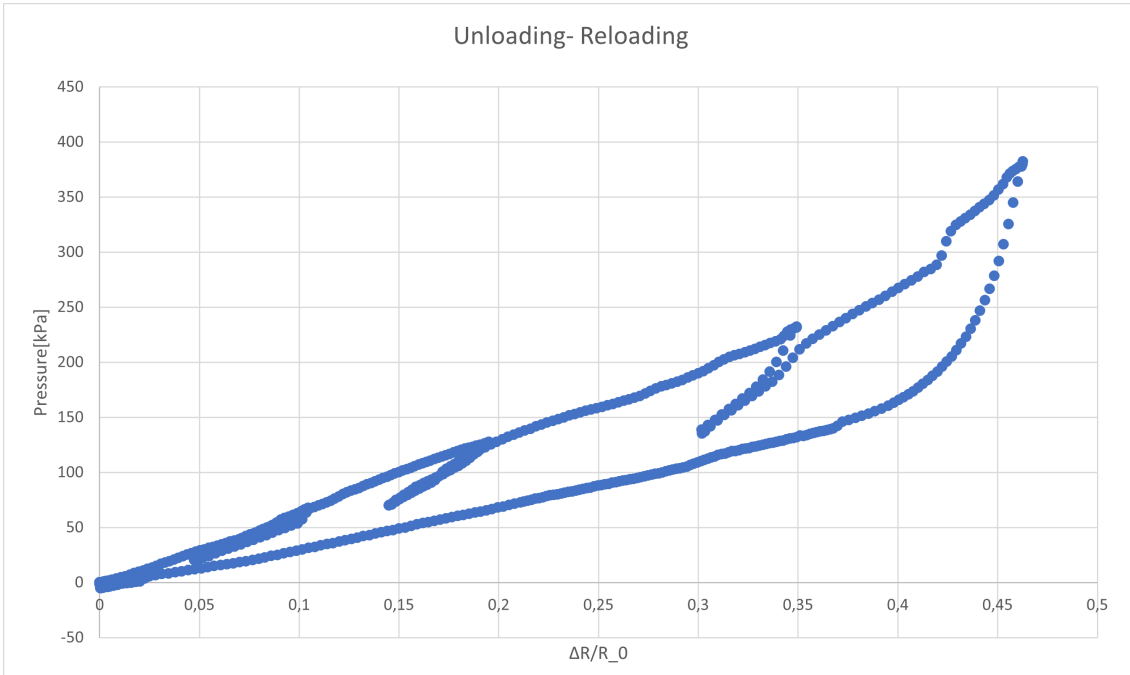


Figure 4.24: Plot of unloading reloading loops test 4, on the y-axis the pressure P [kPa] inside the pressuremeter and on the x-axis $\epsilon_\theta = \frac{\Delta R}{R_0}$

Table 4.1: Shear modulus $G_{U_{ncorr}}$ calculated from uncorrected unloading-reloading loops from pressuremeter test in soil

	Test 1	Test 2	Test 3	Test 4
G_{ur} from loop 1	0.540 MPa	0.404 MPa	0.424 MPa	0.356 MPa
G_{ur} from loop 2	1.127 MPa	0.562 MPa	0.565 MPa	0.556 MPa
G_{ur} from loop 3	-	-	1.195 MPa	0.758 MPa
G_u from unloading at 50% strain	3.974 MPa	2.942 MPa	4.014 MPa	3.165 MPa

4.2.2 Correction factor from tests in air

The stiffness of the pressuremeter itself was found by performing the unloading and reloading of the device without any resistance other than the atmospheric pressure shown in Figure 4.25. That graph was expected to be almost linear since the membrane is made of rubber. Since the graph was showing some in-elastic behavior, it was assumed that the viscoelastic properties of rubber came into play. This means, the tests were done a bit fast, and it made the rubber show stiffer properties due to the viscos effect. Considering the fact that, the main tests were done at a lower rate, then the viscous effect is expected to disappear, and only the elastic effect will remain. This means we can use the stiffness of the last unloading part, as shown in the Figure 4.25), for correction. Equation 4.1 shows the correction factor calculated from the results and was used to correct the measurements made by the pressuremeter.

$$P[kPa] = 368.71 \cdot \frac{\Delta R}{R_0} \quad (4.1)$$

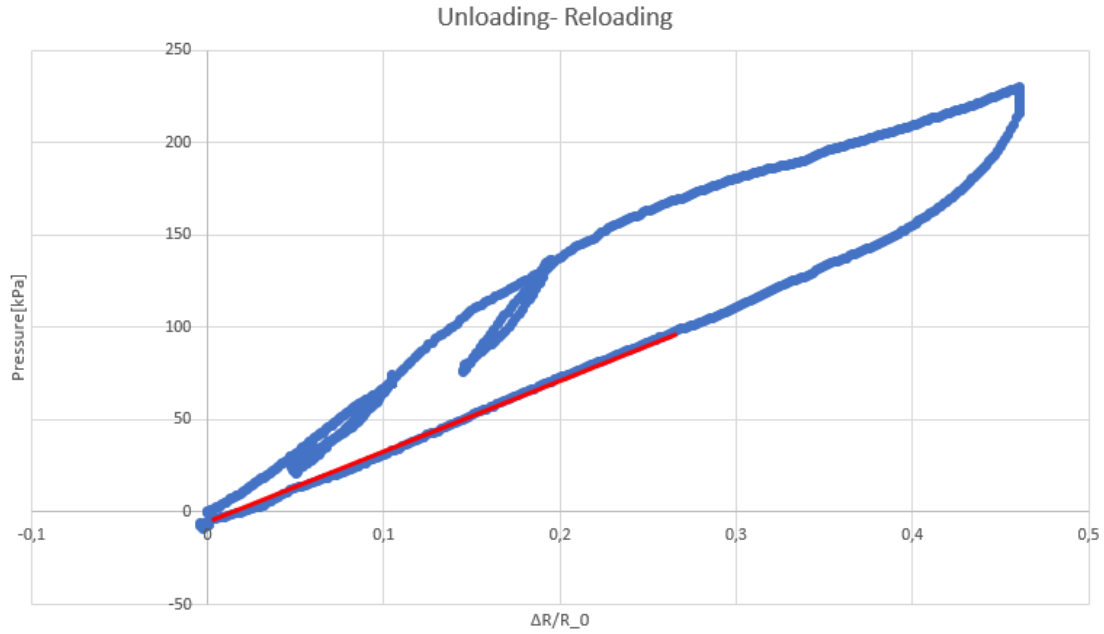


Figure 4.25: Plot of unloading reloading loops, on the y-axis the pressure P [kPa] inside the pressuremeter and on the x-axis $\epsilon_\theta = \frac{\Delta R}{R_0}$

4.2.3 Corrected measurements of shear modulus

The correction factor was applied to the test data and the shear modulus of the soil itself could be found. In total, there were performed 4 test in the soil. Two of them with two loops and two with three loops. The corrected graphs are shown in Figure 4.26, Figure 4.27, Figure 4.28, and Figure 4.29. The interpreted shear modulus G of the 4 tests are shown in Table 4.3

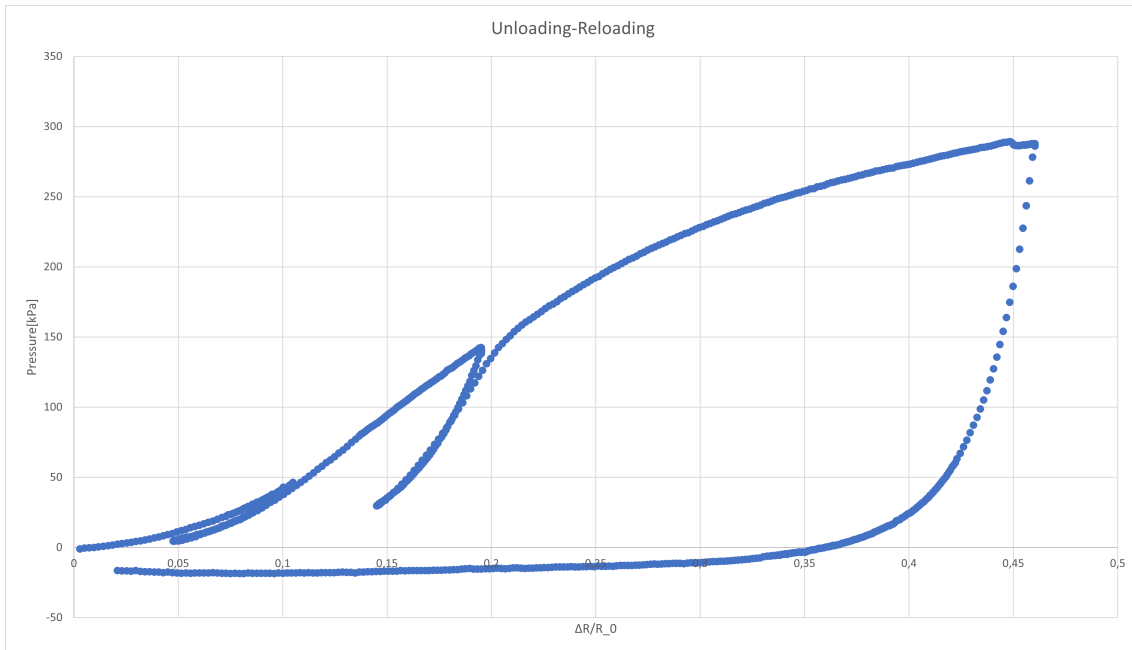


Figure 4.26: Plot of corrected unloading reloading loops, on the y-axis the pressure P [kPa] inside the pressuremeter and on the x-axis $\epsilon_\theta = \frac{\Delta R}{R_0}$

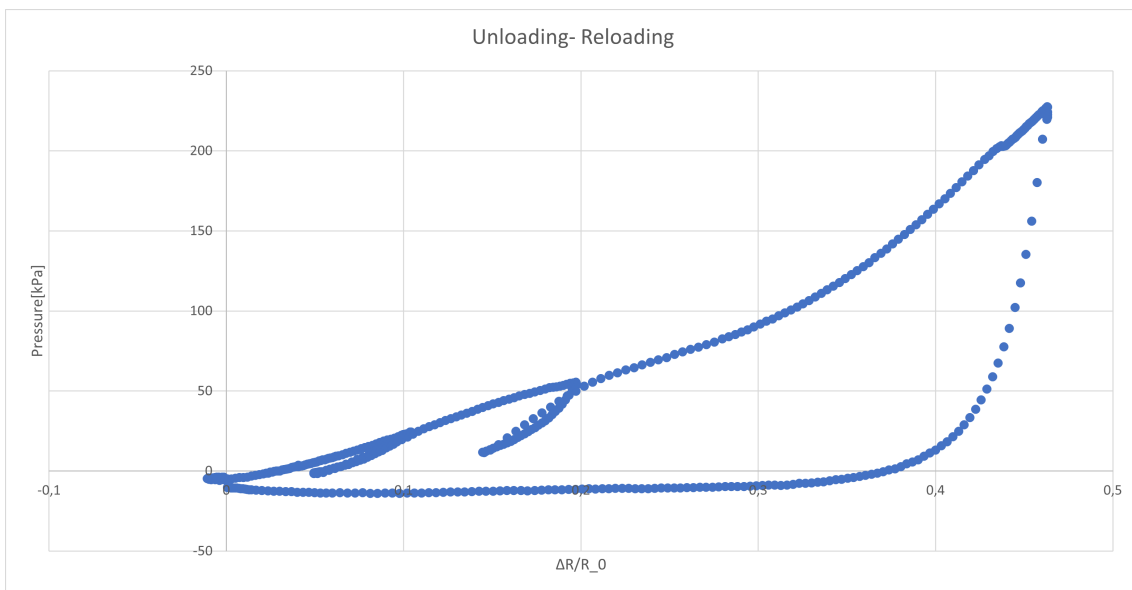


Figure 4.27: Plot of corrected unloading reloading loops, on the y-axis the pressure P [kPa] inside the pressuremeter and on the x-axis $\epsilon_\theta = \frac{\Delta R}{R_0}$

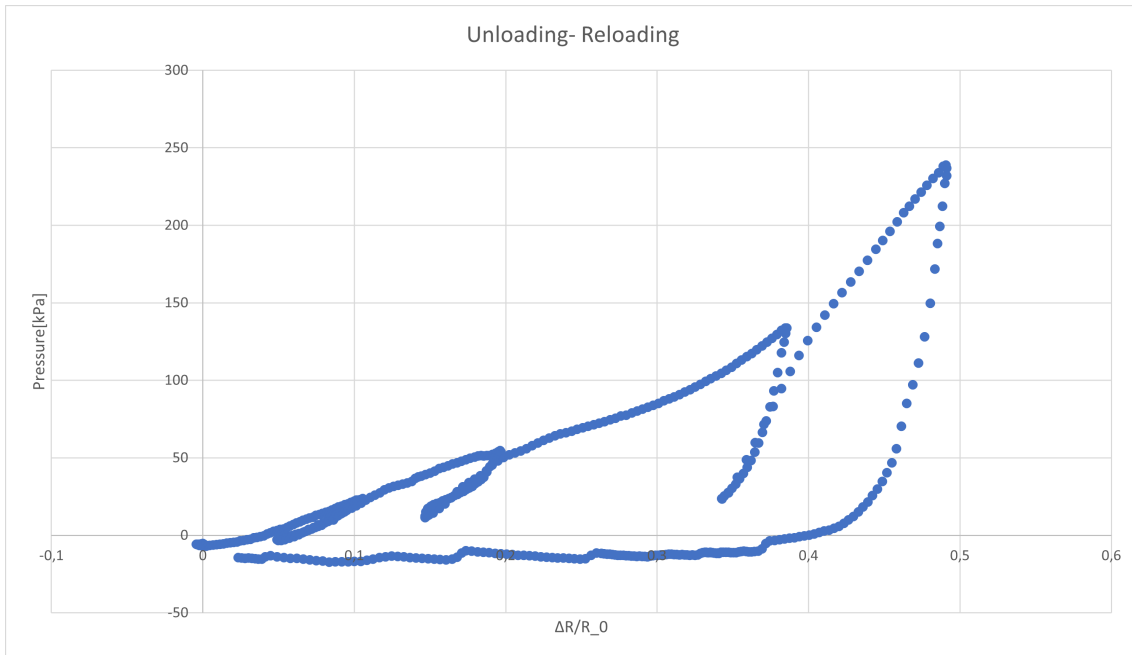


Figure 4.28: Plot of corrected unloading reloading loops, on the y-axis the pressure P [kPa] inside the pressuremeter and on the x-axis $\epsilon_\theta = \frac{\Delta R}{R_0}$

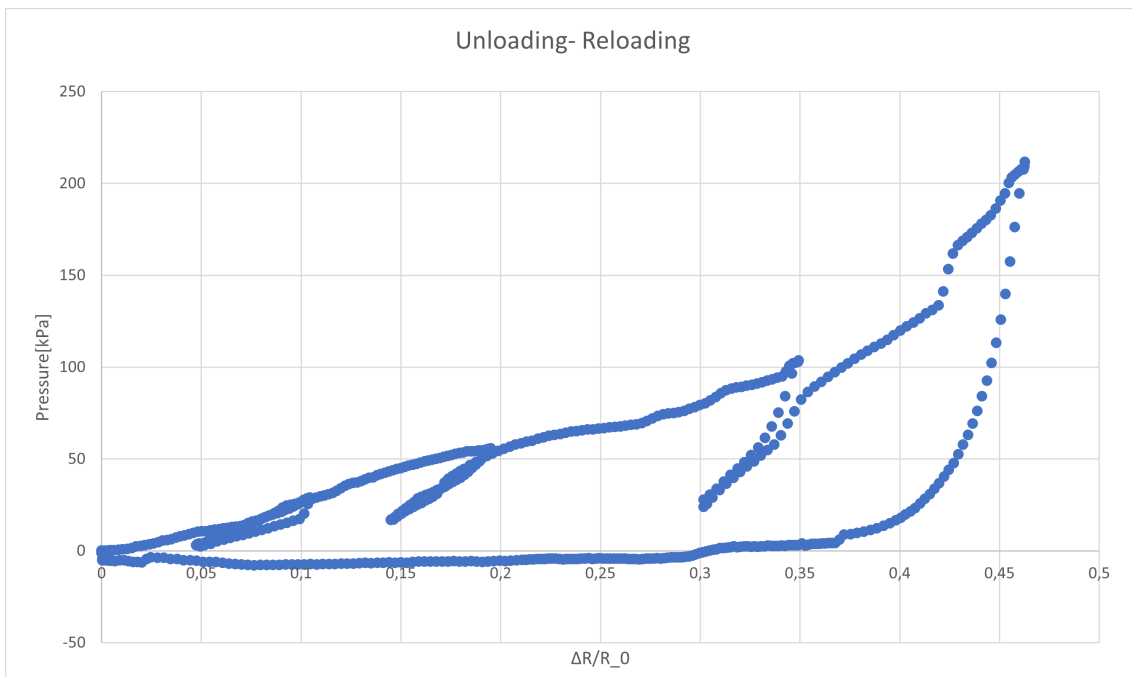


Figure 4.29: Plot of corrected unloading reloading loops, on the y-axis the pressure P [kPa] inside the pressuremeter and on the x-axis $\epsilon_\theta = \frac{\Delta R}{R_0}$

Table 4.2: Shear modulus G_{ur} and G_u calculated from corrected unloading-reloading loops from pressuremeter test in soil

	Test 1	Test 2	Test 3	Test 4
G_{ur} from loop 1	0.349 MPa	0.228 MPa	0.234 MPa	0.214 MPa
G_{ur} from loop 2	0.946 MPa	0.373 MPa	0.383 MPa	0.364 MPa
G_{ur} from loop 3	-	-	0.879 MPa	0.556 MPa
G_u from unloading at 50% strain	3.484 MPa	2.282 MPa	3.023 MPa	3.413 MPa

4.3 Plaxis 2D simulation of pressuremeter

As explained previously the Plaxis simulation was run as one loading-unloading loop. This means that the result from the Plaxis simulation is an Unloading shear modulus G_u . The results from the plaxis simulation are shown in Figure 4.30 and resulted in a G_u of 11.733 MPa.

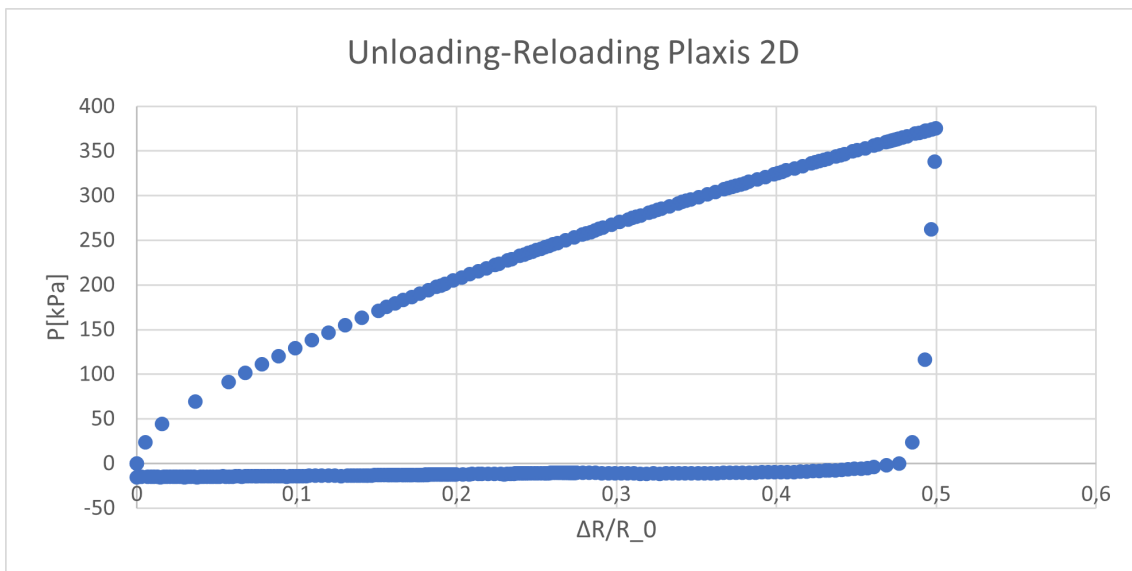


Figure 4.30: Plot of unloading reloading loops, on the y-axis the pressure P [kPa] inside the pressuremeter and on the x-axis $\epsilon_{\theta} = \frac{\Delta R}{R_0}$

4.3.1 Comparison between measured values and Plaxis 2D

The graph from the plaxis simulation and the correct and uncorrected plots of pressure vs. strain from one of the tests in the soil is shown in Figure 4.31.

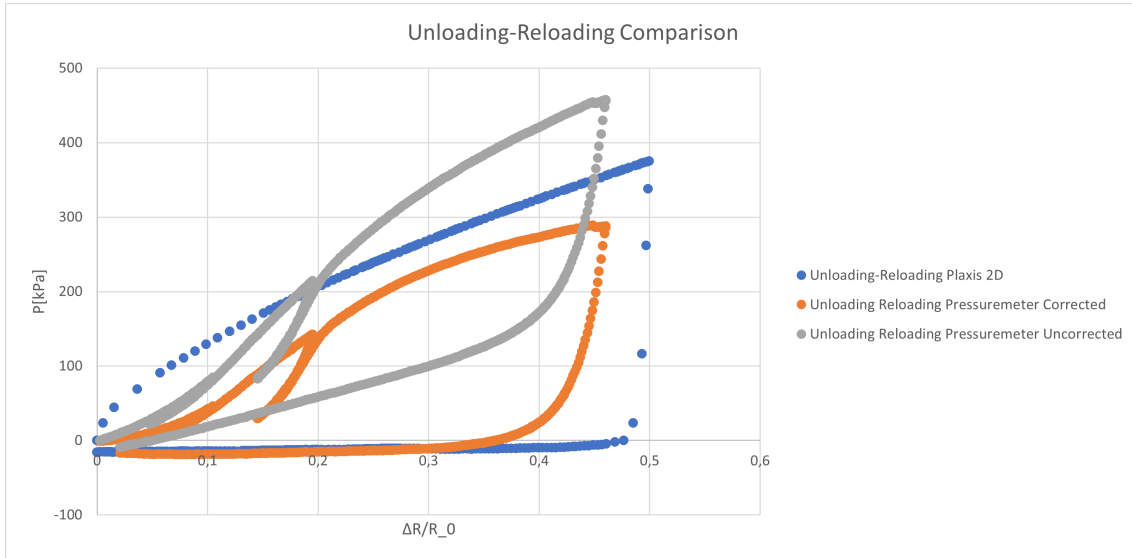


Figure 4.31: Plot of unloading reloading loops, on the y-axis the pressure P [kPa] inside the pressuremeter and on the x-axis $\epsilon_\theta = \frac{\Delta R}{R_0}$

Shear modulus G_u calculated from corrected unloading section at 50% radial strain from pressuremeter tests in soil and the result of the simulation in plaxis is shown in Table 4.1.

Table 4.3: Comparison of shear modulus G_u from all tests

	Test 1	Test 2	Test 3	Test 4	Plaxis2D
G_u at 50% strain	3.484 MPa	2.282 MPa	3.023 MPa	3.413 MPa	11.733 MPa

Table 4.3 shows a large difference in the results of the pressuremeter tests compared to the results from the Plaxis 2D simulation. The shear modulus G_u from Plaxis is 3.85 times larger than the average G_u from the pressuremeter tests.

The shear modulus G_{ur} correlates with the E_{ur} , as shown in Equation 4.2. (Cardoso Bernardes et al. 2022)

$$G_{ur} = \frac{E_{ur}}{2(1 + \nu_{ur})} \quad (4.2)$$

The Stiffness E_{ur}^{ref} was calculated from the Triax test and used as one of the stiffness parameters in the Hardening soil model in Plaxis2D. The E_{ur}^{ref} was a reference stiffness for a p_{ref} value of 100 kPa. To figure out the stiffness of the soil in the large chamber at 1 m depth the stiffness needs to be calculated using the relation in Equation 4.3. (Rebolledo et al. 2019)

$$E_{ur} = E_{ur}^{ref} \cdot \left(\frac{\sigma'_3}{p_{ref}} \right)^m \quad (4.3)$$

Using the values found in Table 2.2 and a depth of 1m σ'_3 equals 5.67 kPa. The expected G_{ur} value for the soil was calculated to be 7.667 MPa combining Equation 4.2 and Equation 4.3.

Chapter 5

Discussion

5.1 Quality of the pressuremeter

The purpose of the initial test was to figure out if the pressuremeter itself was working as it was supposed to. The most critical part of the pressuremeter is the rubber membrane. That membrane is supposed to keep returning to its original state test after test and not experience any plastic deformation. In the tests in the large chamber, the pressuremeter results seem to indicate some viscoelastic behavior in the membrane, which means the tests should be done slowly enough to only have elastic behavior. In the initial test, the membrane was expanded to its recommended limit of 50% radial strain in different ways. As seen in the results from the initial tests the membrane returned to its original state in all of the tests, and it did never show any indication of permanent deformation.

When looking at the shape of the expanded membrane it has a bulbous shape with a slight skew to the right. That was an effect of the points it was measured being slightly closer to the point where the membrane was pinned on the left side. The membrane behaved as expected in both uniformity and elastic behavior for both the Shore 50 and the Shore 70 rubber membrane.

Moving over to the connections and tubes between the pumps and the pressuremeter, the quality there was not good enough. During the initial testing, there were small drops of water coming out of some of the couplings. In those tests, the leaks didn't have an effect on the results because the amount of water wasn't measured. The system was altered to be connected to a new pump during the tests in the large chamber. During those tests, it was difficult to notice any leaks since most of the system was buried in sand.

The effect of the leakage was that the system was not able to hold pressure for an extended period of time as shown in Figure 5.1 for the initial tests. The holding test during the initial tests was performed at a pressure of about 1.2 Bar in a system made to be able to hold a pressure of 16 Bar. That flaw will have a great deal to say for tests at high pressure or tests that last a long time.

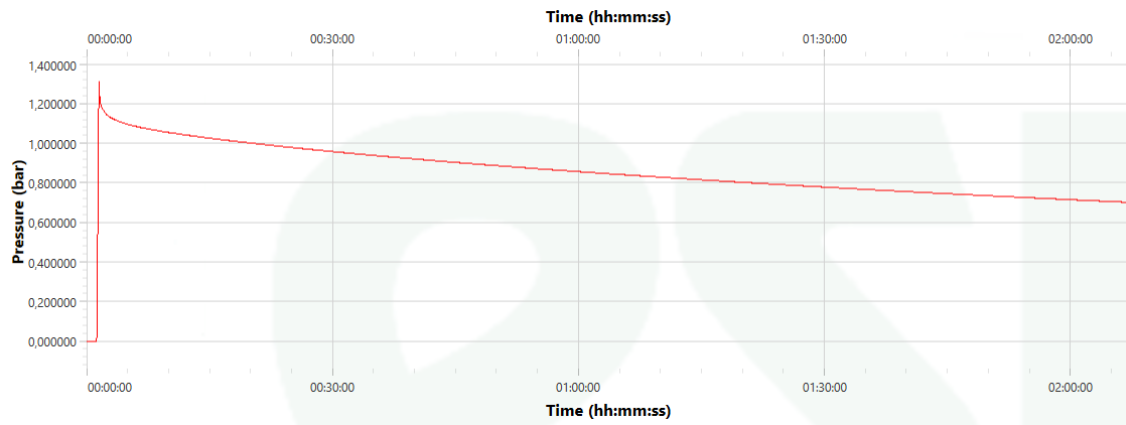


Figure 5.1: Measurement of pressure over time inside the pressuremeter while the chamber was being filled with sand

A holding test for the new system in the large chamber was also performed for about 15 min as is shown in Figure 5.2. That system was able to hold the pressure to a more satisfactory degree than in the initial tests. Considering the pressure being measured in the pump and not inside the pressuremeter, the peak at the start of the test can be explained by some delay in the system and the rate of expansion. The holding test in the large chamber also shows a decrease in pressure over time. It was not as severe as the one in the initial tests, but it will have affected the results to some degree as well.

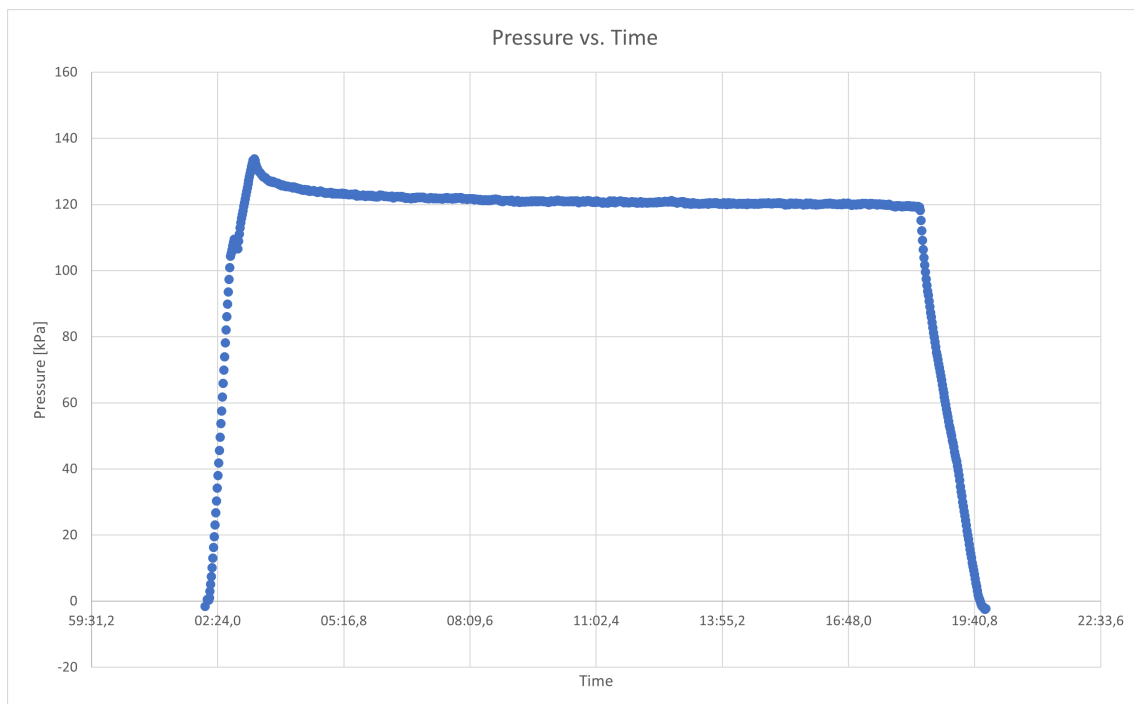


Figure 5.2: Measurement of pressure over time inside the pressuremeter

Figure 5.3 shows a graph, from the pressuremeter being tested in air, in which the rubber of the pressuremeter seems to be deforming in-elastically(viscoelastically) at

some points. It can be seen as the inclination of the graph increases and then decreases at a higher pressure. If plastic deformation were the case, the pressuremeter would not have returned to its original shape. Since all the initial test presented indicates a totally elastic material, it is fair to assume that what looks like viscous effect deformation came from the rubber being deformed too rapidly. Rubber is a viscoelastic material and the increased stiffness is an effect of the molecular structure of rubber, in which the friction between the molecules increases depending on the rate of strain. (Store norske leksikon 2023) Some of the force from the increased pressure will, as an effect of that, be converted into thermal energy. That gave the higher increase in pressure that can be seen in some sections of the graph.

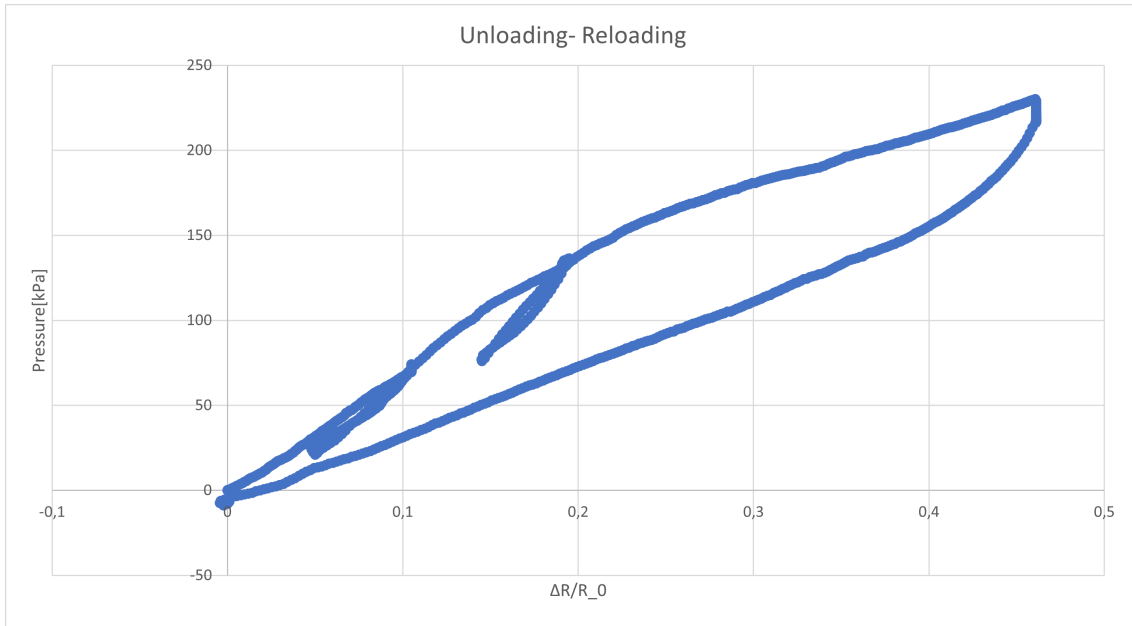


Figure 5.3: Plot of unloading-reloading loops in air, on the y-axis the pressure P [kPa] inside the pressuremeter and on the x-axis $\epsilon_\theta = \frac{\Delta R}{R_0}$

5.2 Accuracy of measurements

The pressuremeter tested in this thesis was a prototype of a more advanced model that will be attached to the back of the CPT probe. The advanced model will be able to measure the displacement of the membrane at multiple points instead of just measuring the volume of water injected into the system. The problem with just measuring the volume injected was that there was no way of knowing how the membrane expanded when it was underground. That means there is no way of knowing the radial strain. Assuming it to be expanding as a perfect cylinder, as has been done here, would give large margins of error.

The leakage experienced during the testing would have given some loss in pressure during the tests. The effect of the leakage was hard to quantify since the pressuremeter was buried in the ground. The viscoelastic properties did influence the pressure measured in the tests, as previously discussed, but to what extent it affected

the tests is hard to say without further tests.

There was a large difference between the shear modulus G_{ur} calculated from the hardening soil parameters and the G_u interpreted from the Plaxis2D simulation results. It can be explained by the fact that the shear modulus G_{ur} is defined as the average inclination of the unloading reloading loop and that the G_u from the plaxis results was interpreted from the steepest section of the unloading part of the graph. What can't be explained in the same manner was why the G_u from the plaxis simulation was 3.85 times larger than the average G_u from the pressuremeter tests.

Sedran et al. 2019 proposes that there is a correlation between the Menard modulus E_M and Young's modulus E . Where the Menard modulus was the stiffness measured using a pressuremeter and using $\nu = 0.33$ to convert the measured G_{ur} to E_M . The correlation that was proposed to be Equation 5.1 where the value of α was somewhere between $\frac{1}{4}$ and one. The value of alpha was very much dependent on the horizontal stress at the depth at which the pressuremeter test was taken, and the value of α got closer to one as the horizontal stress got closer to zero. In the tests performed in this thesis, the horizontal stress was very close to zero, at around 6 kPa, indicating that the value of α should be close to one. It can be concluded that the effect of this correlation factor, in this case, was almost nonexistent and could only account for a small deviation from the predicted value. To figure out if the measured values of the shear modulus had some correlation to the predicted shear modulus from the Hardening soil parameters it would have been necessary to do more tests at different depths.

$$E = \frac{E_M}{\alpha} \quad (5.1)$$

The correction factor interpreted from the pressuremeter test in air was 369 kPa times the radial strain. The correction factor at 50% strain was 40% of the measured pressure during the test in soil. In this case, when testing at such a low depth, this correction factor had a lot of influence on the results. Considering there were made a number of assumptions on the interpretation of the correction factor, this was another large margin of error and greatly contributed to the result being so far off the predicted value.

The large difference between the predicted shear modulus G_{ur} and the measured value can be explained by the large amounts of error connected to the testing of the pressuremeter as explained above.

Chapter 6

Conclusion

In this study, the quality of the pressuremeter system and the accuracy of measurements obtained from pressuremeter testing were evaluated. The findings provided insights into the behavior of the rubber membrane, the performance of the connections and tubes, and the overall reliability of the pressuremeter.

The results indicated that the rubber membrane of the pressuremeter exhibited satisfactory behavior, returning to its original state without undergoing plastic deformation. This is a critical aspect as it ensures the accuracy and repeatability of the measurements. However, issues were identified with the connections and tubes, leading to small leaks. These leaks compromised the system's ability to hold pressure for extended periods, which can be problematic in high-pressure tests or tests conducted over a long duration. Addressing these quality concerns is essential to enhance the reliability of the pressuremeter system.

The accuracy of measurements obtained from the pressuremeter tests was subject to various factors. The prototype pressuremeter used in this study measured the volume of water injected into the system, which required assumptions about the radial strain and the expansion of the rubber membrane. Deviations from these assumptions introduced uncertainties and potential errors in the calculated soil parameters. Additionally, the presence of leaks and the viscoelastic properties of the rubber material affected the pressure measurements. Further research is needed to quantify the precise impact of these factors and improve the accuracy of pressuremeter measurements.

The comparison between the calculated shear moduli from soil parameters and those interpreted from Plaxis2D simulation results revealed discrepancies. This suggests the need for further investigations and more extensive testing at different depths to establish correlations and improve the understanding of the soil's mechanical behavior.

In conclusion, while the rubber membrane of the pressuremeter demonstrated satisfactory behavior, improvements are required in the connections and tubes to eliminate leaks and enhance the system's ability to hold pressure. The accuracy of measurements can be improved by addressing assumptions about the radial strain

and the expansion of the rubber membrane. Further research and testing are necessary to establish correlations between measured and simulated shear moduli and to refine the interpretation of pressuremeter data for reliable geotechnical design.

Chapter 7

Recommendation for further work

7.1 Leakage

There is a need for a more robust and secure connection between the pressuremeter and the pump. The pressuremeter relies on accurate measurement of volumetric change and leakage has a great impact on those results. The system needs to be upgraded and the upgrades needs to be confirmed with holding tests (tests where the an increased volume is held constant and registering how the pressure changes over time).

7.2 Rate of volumetric change

The pressuremeter tests require some boundaries of how fast the volume of the pressuremeter can be changed. As discussed in the thesis the rubber experienced an increase in stiffness because the tests happened too fast. This can be done by performing tests at different speeds and comparing the results. A maximum limit should be determined from the results where there is a minimal effect of the viscous properties of the rubber membrane.

7.3 Correlation factor

Is there a correlation factor between measured shear modulus using the pressuremeter and share modulus from Triax and Oedometer? Performing a large number of tests at different horizontal stress and comparing this to the Triax and Oedometer results at the same horizontal stress might unveil a correlation factor.

Bibliography

- Cardoso Bernardes, H. et al. (2022). ‘Coupling hardening soil model and Ménard pressuremeter tests to predict pile behavior’. eng. In: *European journal of environmental and civil engineering* 26.11, pp. 5221–5240. ISSN: 1964-8189.
- Clarke, B. G. (1997). ‘Pressuremeter testing in ground investigation .2. Interpretation’. eng. In: *Proceedings of the Institution of Civil Engineers. Geotechnical engineering* 125.1, pp. 42–52. ISSN: 1353-2618.
- Mehdi-Ahmadi, M. and P. Karambakhsh (2009). ‘A numerical study of the effects of calibration chamber boundary conditions on pressuremeter test results in sand’. In: *GeoHalifax 2009*.
- Plaxis 2D* (2023). Accessed: 2023-05-31. Bentley Systems. URL: <https://www.bentley.com/software/plaxis-2d/> (visited on 31st May 2023).
- Rebolledo, Juan Félix Rodríguez, Raimundo Francisco Pérez León and José Camapum de Carvalho (2019). ‘Obtaining the Mechanical Parameters for the Hardening Soil Model of Tropical Soils in the City of Brasília’. eng. In: *Soils and Rocks* 42.1, pp. 61–74. ISSN: 1980-9743.
- Sedran, G., R. Failmezger and A. Drevininkas (Sept. 2019). ‘Relationship between Menard EM and Young’s E moduli for cohesionless soils’. In.
- Søvik, Marius Mathisen (2017). *Macro-model description and model verification*. eng. URL: <http://hdl.handle.net/11250/2457824>.
- Store norske leksikon (2023). *Viskoelastisitet*. URL: <https://snl.no/viskoelastisitet> (visited on 26th May 2023).
- Winter, E. (1987). ‘Pressuremeter in geotechnical practice’. eng. In: *International journal of rock mechanics and mining sciences and geomechanics abstracts* 24.6, pp. 11–16. ISSN: 0148-9062.



 **NTNU**

Norwegian University of
Science and Technology